Novel Semi-Active Suspension with Tunable Stiffness and Damping Characteristics

by

Adrian Wong

A thesis
presented to the University of Waterloo
in fulfillment of the
thesis requirement for the degree of
Master of Applied Science
in
Mechanical Engineering

Waterloo, Ontario, Canada, 2012

I hereby declare that I am the sole author of this thesis. This is a true copy of the thesis, including any required final revisions, as accepted by my examiners.

I understand that my thesis may be made electronically available to the public.

Abstract

For the past several decades there have been many attempts to improve suspension performance due to its importance within vehicle dynamics. The suspension system main functions are to connect the chassis to the ground, and to isolate the chassis from the ground. To improve upon these two functions, large amounts of effort are focused on two elements that form the building blocks of the suspension system, stiffness and damping. With the advent of new technologies, such as variable dampers, and powerful microprocessors and sensors, suspension performance can be enhanced beyond the traditional capabilities of a passive suspension system. Recently, Yin *et al.* [1, 2] have developed a novel dual chamber pneumatic spring that can provide tunable stiffness characteristics, which is rare compared to the sea of tunable dampers. The purpose of this thesis is to develop a controller to take advantage of the novel pneumatic spring's functionality with a tunable damper to improve vehicle dynamic performance.

Since the pneumatic spring is a slow-acting element (i.e. low bandwidth), the typical control logic for semi-active suspension systems are not practical for this framework. Most semi-active controllers assume the use of fast-acting (i.e. high bandwidth) variable dampers within the suspension design. In this case, a lookup table controller is used to manage the stiffness and damping properties for a wide range of operating conditions.

To determine the optimum stiffness and damping properties, optimization is employed. Four objective functions are used to quantify vehicle performance; ride comfort, rattle space (i.e. suspension deflection), handling (i.e. tire deflection), and undamped sprung mass natural frequency. The goal is to minimize the first three objectives, while maximizing the latter to avoid motion sickness starting from 1Hz and downward. However, these goals cannot be attained simultaneously, necessitating compromises between them. Using the optimization strength of genetic algorithms, a Pareto optima set can be generated to determine the compromises between objective functions that have been normalized. Using a trade-off study, the stiffness and damping properties can be selected from the Pareto optima set for suitability within an operating condition of the control logic.

When implementing the lookup table controller, a practical method is employed to recognize the road profile as there is no direct method to determine road profile. To determine the road profile for the lookup table controller, the unsprung mass RMS acceleration and suspension state are utilized. To alleviate the inherent flip-flopping drawback of lookup table controllers, a temporal deadband is employed to eliminate the flip-flopping of the lookup table controller.

Results from the semi-active suspension with tunable stiffness and damping show that vehicle performance, depending on road roughness and vehicle speed, can improve up to 18% over passive suspension systems. Since the controller does not constantly adjust the damping properties, cost and reliability may increase over traditional semi-active suspension systems. The flip-flopping drawback of lookup table controllers has been reduced through the use of a temporal deadband, however further enhancement is required to eliminate flip-flopping within the control logic. Looking forward, the novel semi-active suspension has great potential to improve vehicle dynamic performance especially for heavy vehicles that have large sprung mass variation, but to increase robustness the following should be considered: better road profile recognition, the elimination of flip-flopping between suspension states, and using state equations model of the pneumatic spring within the vehicle model for optimization and evaluation.

Acknowledgements

Completing this thesis on a part-time basis has been a long journey. To start, I would like to thank my colleagues at General Dynamics Land Systems Canada for their support. In particular, I would like to extend my gratitude to Dr. Xiong Zhang, Dr. Ayhan Ince, Zeljko Knezevic, and Phong Vo for their knowledge and valuable experience.

To my friends, thank you for keeping my spirits up and making me laugh. To the Brians, thank you truly for keeping it real.

To my thesis readers, Dr. Steven Lambert and Dr. John McPhee, I thank you greatly for your valuable input and experience. Your critiques have helped to improve the quality of my thesis.

To my thesis supervisor, Dr. Amir Khajepour, I must express to you how truly grateful and appreciative I am of your mentorship, kindness, and patience you have shown me during my studies. This thesis would have never emerged without your guidance and experience. I am truly indebted for accepting me as your student.

To my parents, in-laws, and Eugene, thank you for your loving support and encouragement. I love you guys.

Lastly and most importantly, to my beautiful wife, thank you for your enduring strength and love you have given me throughout this entire journey. Words cannot express my love and appreciation for you. Thank you for the greatest gift, our daughter. This thesis is dedicated to you.

Table of Contents

List of Figures

List of Tables

Chapter 1

Introduction

For the past several decades, many attempts have been made to improve vehicle performance by means of improving the suspension system. From a high-level perspective, most suspension systems comprise of three basic elements; spring, damper, and linkages. Each of these elements has their own functional purpose within the suspension system; the spring element provides energy storage, the damping element provides energy dissipation, and the linkages provide mechanism constraints on the suspension motion. Together, the composition of these functions allows the suspension system to achieve its main purpose which is to maintain contact between the road and tires and to isolate the chassis from road-induced vibrations. Of the three basic elements, the spring and damper are the most studied elements within the suspension system because of their simple functionality and their considerable influence on vehicle dynamic performance.

Overall, ride comfort, rattle space, and handling are the most frequent used metrics for evaluating vehicle dynamic performance [3]. Ride comfort is proportional to the absolute acceleration of the vehicle body, while rattle space and handling are linked to the relative displacement between the vehicle body and wheels/tires and between the wheels/tires and road, respectively. The main challenge in suspension design is achieving improvement in all three objectives since these objectives will likely conflict with each other [4], as is shown in subsequent sections. However, with the advent of active elements and the computing power and prevalence of microprocessors, the challenge in improving all three objectives becomes more realizable.

Since there is extensive literature for the improvement of suspension systems as a whole, the following sections presents a progressive overview of the strategies and elements used to improve the suspension systems performance, followed by the thesis objective and scope.

1.1 Passive Suspension

Passive suspension systems (i.e. conventional suspension systems) consist of a spring, which can be for example a coil spring or air spring, and a damper, which can be for example the hydraulic flow resistance through an orifice. In addition, it is characterized by the absence of any active elements or electronics. Although there have been many attempts to use parametric non-linear springs and dampers, the limitations of passive suspension systems nevertheless persist because of these inert elements. Hence, the design and synthesis of a passive suspension system requires experienced engineers to make compromises between a variety of vehicle performance metrics to obtain the desired vehicle dynamic performance to satisfy various operational requirements. The prevalence of passive suspension systems within most automobiles stems from their design simplicity and reliability and their low associated manufacturing cost. Thus, these factors make them attractive relative to more advanced suspension systems [5].

1.1.1 Suspension Tuning

To select the springs and dampers of the passive suspension system, various techniques have arose to assist engineers in the selection process and comprehension of the compromises that are produced from the selected properties. Early investigations involved employing trade-off studies to determine the spring and damper properties of the passive suspension system. However, there are drawbacks using trade-off studies for determining the spring and damping properties. Trade-off studies require large amounts of experiments to reasonably determine the spring and damping properties, which also incurs large costs, and the results may not be global optimal solutions. Evolving from trade-off studies is the design of experiments (DOE) method which provides a systematic approach for performing a trade-off study. Using the DOE systematic approach allows engineers to determine interactions between parameters and perform sensitively analyses. However, because DOEs evolved from trade-off studies, the drawbacks are similar to trade-off studies.

To overcome the limitations associated with DOEs and trade-off studies, engineers have been employing mathematical optimization techniques more frequently for the selection of spring and dampers properties. There are two main mathematical optimization approaches that have been employed for selecting the optimal suspension properties, gradient and stochastic based. In general, gradient based optimization uses gradients vectors of the objectives with respect to the design space

to find the optimal results, while stochastic based optimization uses the fitness of random variables across the design space to find optimal results. Many studies that used gradient based optimization [6, 7, 8, and 9] with success found that the results are sensitive to the initial conditions, which means that gradient based optimization are sensitive to local minimums or maximums. Additionally, these studies found that the results from gradient based optimization are sensitive to the number of design variables considered, the quality of the gradients approximated from the objectives (i.e. well-defined versus ill-defined functions) , and numerical noise, which are inherent in complex numerical models. Lastly, gradient based optimization produces a single solution set from an aggregate of objectives within the design space.

Lately, more studies [10, 11, 12, and 13] have gravitated toward the use stochastic based optimization for determining the optimal spring and damping parameters. The gravitation towards stochastic based optimization comes from studies, such as Baumal *et al*. [14], that prove that stochastic based optimization is better than gradient based optimization for this class of problem. A variety of algorithms fall into the stochastic based optimization class including genetic algorithms (GA) and simulated annealing. The shift towards the stochastic based optimization for finding optimal solutions comes from the following:

i. insensitivity to number of design variables (i.e. size of design space)
ii. insensitivity to the complex (i.e. ill-defined) objectives
iii. perform global search within design space
iv. ability to produce non-dominated solutions (i.e. Pareto optima set) for multiobjective problems

The last point favouring the stochastic based-optimization is important because the Pareto optima set allows engineers to analyze all the optimal solutions and understand the compromises between each optimal solution. The main drawback of stochastic based optimization is the large computation expense required to find the solutions.

1.2 Semi-Active Suspension

Semi-active suspension systems are generally classified as suspension systems whose active elements are adjustable springs and/or dampers. To date, most of the advancement in semi-active suspension systems has been made through the use of adjustable dampers. The various design techniques used to achieve adjustable damping, include:

- Position controlled valves, such as solenoid valves
- Electro and Magneto-rheological (ER) fluids

In all cases, modulating the damping properties requires a small power source, but does not introduce energy into the suspension system. Compared to passive suspension systems, their designs are more complex, they have reduced reliability, and are relatively more expensive to manufacture. Overall however, the impact of semi-active suspension systems on vehicle dynamics performance surpasses the performance that passive suspension systems can achieve and has been used on luxury automobiles.

1.2.1 Controller Designs

To achieve the enhancement of vehicle dynamic performance using the added functionality from the above active elements requires a controller to manage their properties. Without the controller to manage their properties, the semi-active suspension system would regress to a passive suspension system. In general, the primary function of controllers is to manage and regulate system properties based on the system states, which is obtained usually through feedback means, to reach the desired output response. Depending on the controller strategy employed, the degree of enhancement in terms of vehicle performance over passive suspension systems can vary. The following sections describe some conventional and new control strategies used for managing damping properties.

1.2.1.1 Skyhook Controller

Skyhook control is a proposed control strategy by Crosby and Karnopp [15] to manage the damping properties. The heart of the control strategy is to assume a fictitious damper, c_{sky}, connected to the sky that controls the attitude of the vehicle body shown in Figure 1-1a. The damping force that is

generated from the fictitious damper, c_{sky}, is always in the direction opposite to the absolute velocity of the body. For implementation purposes, the fictitious damper is replaced by a variable damper as shown in Figure 1-1b. The control logic using the variable damper, c_{sky}, for a 2 DOF is as follows:

$$c_{sky} = \begin{cases} c_{max} & \dot{x_2}(\dot{x_2} - \dot{x_1}) \geq 0 \\ 0 & \dot{x_2}(\dot{x_2} - \dot{x_1}) < 0 \end{cases} \quad \textbf{(1.1)}$$

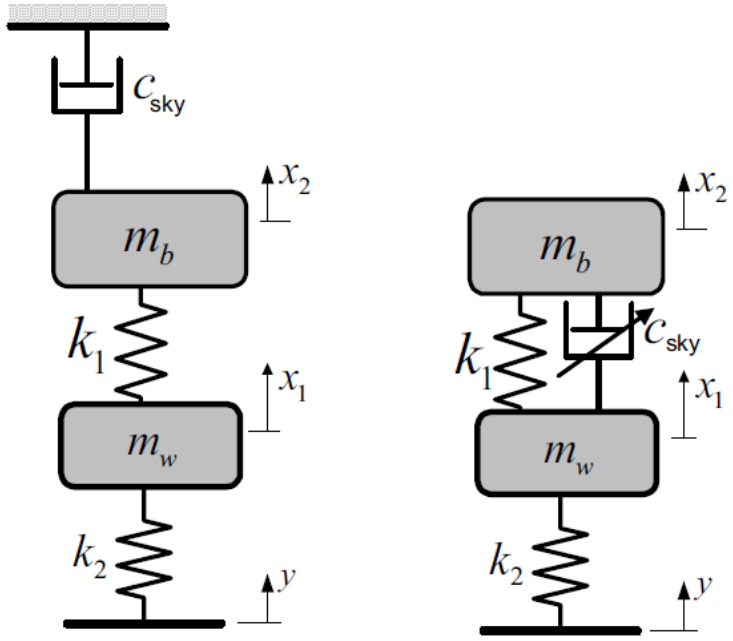

a) Idealized Skyhook Damper b) Application of Skyhook Damper

Figure 1-1: Schematic of Skyhook *(Eslaminasab N., 2008) [16]*

Practical implementation of the Skyhook control is challenging since the ability to measure absolute velocity is often difficult.

1.2.1.2 Groundhook Controller

Groundhook control is similar to Skyhook control except the fictitious damper is connected to ground for the purpose of controlling the attitude of the wheels as shown in Figure 1-2 [16]. The damping force that is generated from the fictitious damper, c_{Gr}, is always in the direction opposite to the

absolute velocity of the wheel. Implementation is similar to the Skyhook implementation shown in Figure 1-1b. The control logic using the variable damper for a 2 DOF is as follows:

$$c_{Gr} = \begin{cases} 0 & \dot{x_1}(\dot{x_2} - \dot{x_1}) \geq 0 \\ c_{max} & \dot{x_1}(\dot{x_2} - \dot{x_1}) < 0 \end{cases} \quad \textbf{(1.2)}$$

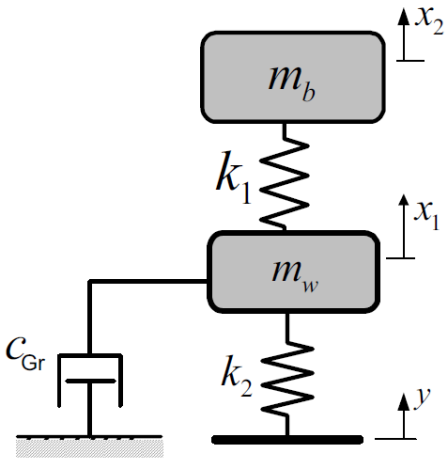

Figure 1-2: Schematic Groundhook Damper *(Eslaminasab N., 2008) [16]*

Groundhook control faces similar implantation challenges as the Skyhook control since the control logic requires measuring absolute velocity of the wheels.

1.2.1.3 Frequency Estimated-Based Controller

Lozoya-Santos, et.al [17] developed a control strategy which uses a lookup table to obtain the desired vehicle performance based on estimates of the road frequency. The outputs of the lookup table control logic are the optimal damping properties, which are determined off-line with respect to the vehicle performance objectives. Using a moving window, the average road frequency can be estimated using the root mean square (RMS) of the damper piston deflection and velocity as given by:

$$\hat{f} = \frac{\dot{z}_{rms}}{2\pi z_{rms}} \quad \textbf{(1.3)}$$

where,

z_{rms} and $\dot{z}_{rms}$ are the deflection and velocity of the damper piston, respectively

$\hat{f}$ is the estimated average road frequency

In terms of performance, the lookup table controller improved upon all the objectives relative to the passive suspension system.

Comparing this control strategy overall to the Skyhook and Groundhook controllers reveals that this control strategy does not require absolute velocity, and that this control strategy is suitable for slow-active (i.e. low bandwidth) elements. This suitability towards slow-active element exists because changes in damping properties, which are based on a moving window evaluating road frequency, are infrequent relative to Skyhook and Groundhook control.

1.3 Active Suspension

Active suspension systems are characterized by the substitution of the spring and damper elements of a passive suspension system with a force actuator, which can be hydraulic, electro-mechanic, pneumatic or magnetic. Furthermore, active suspension systems require a series of sensors such as an accelerometer, force transducer, displacement transducer to function. Relative to the semi-active suspension system, the force actuator of the active suspension introduces energy into the system, which leads to large power consumptions compared to the semi-active suspension system. In addition to the drawback of large power consumption, active suspension design is very complex and manufacturing is expensive. Even though active suspension systems can achieve the best suspension performance compared with passive suspension and semi-active suspension, its drawback has limited their appeal.

1.4 Novel Dual Chamber Pneumatic Spring

Recently, a novel pneumatic spring has been introduced by Yin el.al [1, 2]. Employing a dual chamber pneumatic cylinder, in which the pressure of each chamber can be controlled independently, this element has the ability to provide tunable stiffness and variable ride height under various operation conditions and especially when large variations in sprung mass (i.e. heavy trucks) are involved. The schematic of the dual chamber pneumatic spring is presented in Figure 1-3.

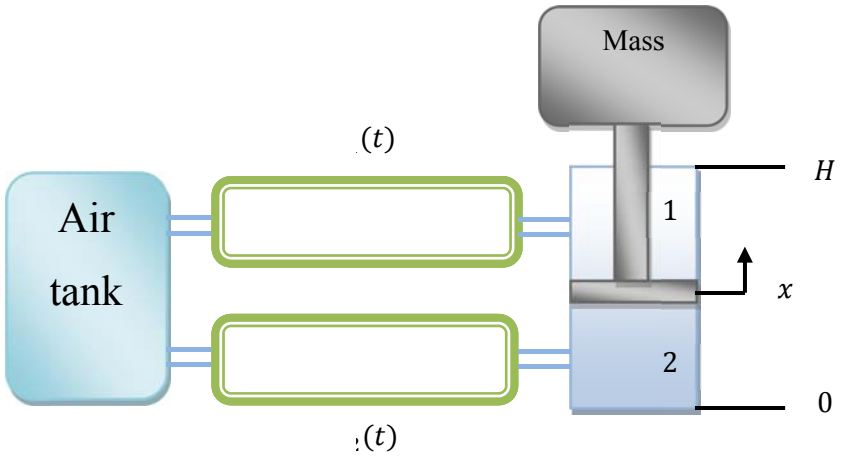

Figure 1-3: Schematic of Dual Chamber Pneumatic Spring

Preliminary analysis and testing of this spring has shown successfully that a wide range of stiffness values can be achieved. Unlike most adjustable dampers however, the stiffness properties for the spring cannot be tuned quickly. Thus, the dual chamber pneumatic spring is considered a slow-acting (i.e. low bandwidth) element.

1.5 Thesis Motivation and Objective

As shown in the literature review, previous studies have shown great improvement in vehicle dynamic performance through the control of the damping property. Although the adjustment of the damping property can bring about improved vehicle dynamic performance, the stiffness properties of the suspension remains constant and thus the undamped natural frequency remains unchanged. With the novel pneumatic spring, the ability to adjust the suspension stiffness properties independently of the damping property and suspension stroke can be achieved. Using this available functionality in conjunction with a variable damper and combining them with readily availability of microprocessors and sensors, as found on current semi-active suspension systems, suspension properties can be tuned to adapt to varying vehicle mass and road profile inputs.

The primary aim of this thesis is to develop the foundation of a semi-active control logic that adapts spring and damping properties subject to changes in vehicle mass and road condition and to investigate the enhancement in vehicle performance using the developed control logic to manage the

tunable stiffness and damping relative to a passive suspension system. A schematic of the proposed semi-active suspension is presented in Figure 1-4 with the variable spring and damper.

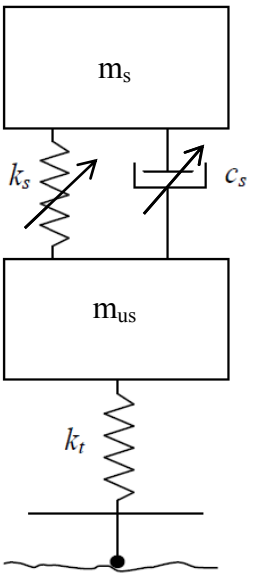

Figure 1-4: Schematic of Proposed Semi-active Suspension with Tunable Spring and Damper

1.5.1 **Scope**

For this thesis, enhancement in vehicle dynamic performance is determined by analytical and numerical means using MATLAB. Throughout the course of this thesis a quarter car model of a mid-sized automobile is used to model the vehicle dynamic performance. Road profile input is determined using ISO 8608, a widely used international standard that provides representation and classification of random road profiles. The effects of non-linear stiffness and damping properties, determining the pneumatic pressure for each chamber, effects of stochastic parameters, and the transitional effects of the adaptive stiffness and damping properties on vehicle performance are beyond the scope of this thesis.

Chapter 2

Vehicle Dynamics Modeling

To assess the effects of stiffness and damping property on vehicle dynamic performance through analytical means, it is necessary to develop:

i) a representative vehicle model, and

ii) a representative road model.

The following sections describe the development of the vehicle model and the road model.

2.1 Vehicle Model

As mentioned in the scope of the thesis, the vehicle model is to be represented by a 2-DOF quarter car model. The quarter car model can be viewed as representing the dynamics on a quadrant of a four wheeled vehicle. Although it may be advantageous to develop a full vehicle model to accurately reflect the vehicle dynamics, the quarter car model provides good approximation of the vertical motion of both the sprung (i.e. chassis) and unsprung (i.e. wheels) mass without the complexity of a full vehicle model. As such, many previous studies [20] have gone on to use the quarter car model for development of semi-active controllers and to determine vehicle performance.

The quarter car model is a system composed of two masses as illustrated in Figure 2-1. The two degrees of freedom for this system are the vertical displacement (x_s and x_{us}) of the sprung and unsprung mass, respectively. The quarter car model is subjected to a base excitation defined by the displacement (r). The displacements x_s, x_{us}, and r are measured from their static nominal positions. The unsprung mass of the system represents the wheel hub and tire and the sprung mass of the system represents a quarter of the chassis mass. Suspension and tire stiffness are denoted by k_s and k_t, while the suspension damping is denoted by c_s. Tire damping in this quarter car model is considered negligible and is not considered in the development of the vehicle model. A free body diagram of the quarter car model is shown in Figure 2-2.

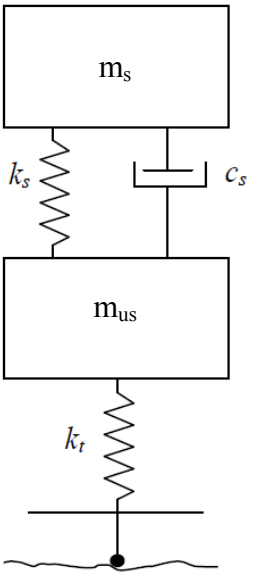

Figure 2-1: Schematic of 2 DOF Quarter Car Model

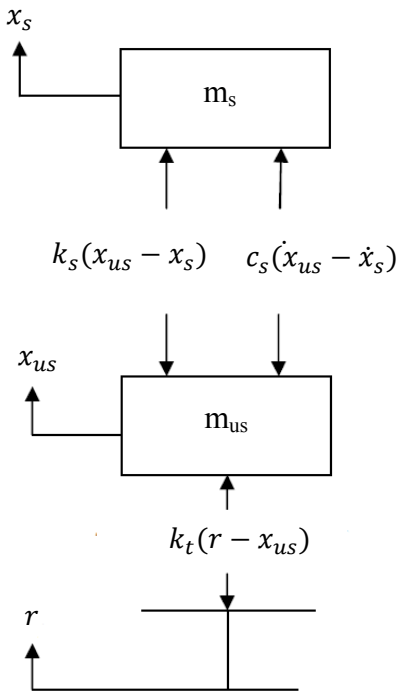

Figure 2-2: Free Body Diagram of 2 DOF Quarter Car Model

Using Newton's second law of motion, the following equations of motion are established:

$$m_s\ddot{x_s} = k_s(x_{us} - x_s) + c_s(\dot{x}_{us} - \dot{x}_s) \quad \textbf{(2.1)}$$

$$m_{us}\ddot{x_{us}} = k_t(r - x_{us}) - k_s(x_{us} - \dot{x_s}) + c_s(\dot{x}_{us} - \dot{x}_s) \quad \textbf{(2.2)}$$

2.1.1 **Frequency Response Function Representation**

An alternative representation of the quarter car model that is used to access the vehicle dynamic performance is through frequency response functions. Frequency response functions (FRF) are transfer functions that capture the spectral outputs, for example acceleration or displacement, relative to its spectral inputs given the existence of a linear input-output relationship. To capture the sprung and unsprung spectral acceleration, velocity, and displacement response from their nominal position, Equation (2.1) and (2.2) is rearranged into:

$$m_s\ddot{x_s} + k_s x_s - k_s x_{us} + c_s\dot{x}_s - c_s\dot{x}_{us} = 0 \quad \textbf{(2.3)}$$

$$m_{us}\ddot{x_{us}} + k_t x_{us} - k_s x_s + k_s x_s + k_s x_{us} - c_s\dot{x}_s + c_s\dot{x}_{us} = k_t r \quad \textbf{(2.4)}$$

Taking the Laplance transform of Equation (2.3) and (2.4) yields the following:

$$m_s s^2 X_s(s) + c_s s X_s(s) + k_s X_s(s) - c_s s X_{us}(s) - k_s X_{us}(s) = 0 \quad \textbf{(2.5)}$$

$$m_{us} s^2 X_{us}(s) + k_t X_{us}(s) + k_s X_{us}(s) + c_s s X_{us}(s) - k_s X_s(s) - c_s s X_s(s) = k_t R(s) \quad \textbf{(2.6)}$$

Rearranging Equation (2.5) and (2.6) into matrix form:

$$\begin{bmatrix} m_s s^2 + c_s s + k_s & -k_s - c_s s \\ -k_s - c_s s & m_{us} s^2 + c_s s + (k_t + k_s) \end{bmatrix} \begin{bmatrix} X_s(s) \\ X_{us}(s) \end{bmatrix} = \begin{bmatrix} 0 \\ R(s)[k_t] \end{bmatrix} \quad \textbf{(2.7)}$$

Evaluating at $s = j\omega$ for Equation (2.7) produces:

$$J(j\omega) \begin{bmatrix} X_s(j\omega) \\ X_{us}(j\omega) \end{bmatrix} = \begin{bmatrix} 0 \\ R(j\omega) \end{bmatrix} \quad \textbf{(2.8)}$$

where,

$$J(j\omega) = \begin{bmatrix} -\omega m_s + j\omega c_s + k_s & -k_s - j\omega c_s \\ \dfrac{-k_s - jwc_s}{k_t} & \dfrac{-\omega^2 m_w + j\omega c_s + (k_t + k_s)}{k_t} \end{bmatrix}$$

Inversing matrix J(jω), the following FRF matrix is obtained for displacement:

$$G(j\omega) = A\begin{bmatrix} \dfrac{-\omega^2 m_w + j\omega c_s + (k_t + k_s)}{k_t} & k_s + j\omega c_s \\ \dfrac{k_s + j\omega c_s}{k_t} & -\omega m_s + j\omega c_s + k_s \end{bmatrix} \quad \textbf{(2.9)}$$

where the determinant is,

$$A = \frac{k_t}{(-\omega^2 m_s + j\omega c_s + k_s)\left(-\omega^2 m_{us} + j\omega c_s + (k_t + k_s)\right) - (-k_s - j\omega c_s)^2}$$

To determine the FRF matrix for velocity and acceleration using the assumption of zero initial conditions, Equation (2.9) is simply multiplied by jω. This multiplication is similar to the single differentiation in Laplace domain in which the transfer function is multiplied by s. The following are the FRF matrix for velocity and acceleration, respectively:

$$G_v(j\omega) = j\omega A\begin{bmatrix} \dfrac{-\omega^2 m_w + j\omega c_s + (k_t + k_s)}{k_t} & k_s + j\omega c_s \\ \dfrac{k_s + j\omega c_s}{k_t} & -\omega m_s + j\omega c_s + k_s \end{bmatrix} \quad \textbf{(2.10)}$$

$$G_a(j\omega) = -\omega^2 A\begin{bmatrix} \dfrac{-\omega^2 m_w + j\omega c_s + (k_t + k_s)}{k_t} & k_s + j\omega c_s \\ \dfrac{k_s + j\omega c_s}{k_t} & -\omega m_s + j\omega c_s + k_s \end{bmatrix} \quad \textbf{(2.11)}$$

To capture the relative displacement response between the sprung mass and unsprung mass and the unsprung mass and road the following relationship is introduced into Equation (2.1) and (2.2):

$$z = x_s - x_{us}$$

$$y = x_{us} - r$$

Using these above relationship, Equation (2.1) and (2.2) is rearranged into:

$$m_s\ddot{z} + c_s\dot{z} + k_s z = -m_s\ddot{x_{us}} \quad \textbf{(2.12)}$$

$$m_{us}\ddot{y} + k_t y - c_t\dot{y} - k_s z - c_s\dot{z} = -m_{us}\ddot{r} \quad \textbf{(2.13)}$$

Performing a Laplance transform on Equation (2.12) and (2.13) yields the following:

$$m_s Z(s) + c_s sZ(s) + k_s Z(s) = -m_s s^2 X_{us}(s) \quad \textbf{(2.14)}$$

$$m_{us}s^2 Y(s) + k_t Y(s) - c_s sZ(s) - k_s Z(s) = -m_{us}s^2 R(s) \quad \textbf{(2.15)}$$

Rearranging Equation (2.14) and (2.15) into matrix and evaluating at $s = j\omega$ gives:

$$K(j\omega)\begin{bmatrix} Z(j\omega) \\ Y(j\omega) \end{bmatrix} = \begin{bmatrix} X_{us}(j\omega) \\ R(j\omega) \end{bmatrix} \quad \textbf{(2.16)}$$

where,

$$K(j\omega) = \begin{bmatrix} \dfrac{-\omega^2 m_s + j\omega c_s + k_s}{\omega^2 m_s} & 0 \\ \dfrac{-k_s - j\omega c_s}{\omega^2 m_{us}} & \dfrac{-\omega^2 m_{us} + k_t}{\omega^2 m_{us}} \end{bmatrix}$$

Inversing matrix K(jω), the following FRF matrix is obtained for relative displacement:

$$H(j\omega) = A\begin{bmatrix} \dfrac{-\omega^2 m_{us} + k_t}{\omega^2 m_{us}} & 0 \\ \dfrac{k_s + j\omega c_s}{\omega^2 m_{us}} & \dfrac{-\omega^2 m_s + j\omega c_s + k_s}{\omega^2 m_s} \end{bmatrix} \quad \textbf{(2.17)}$$

where the determinant is,

$$A = \frac{(\omega^2 m_s)(\omega^2 m_{us})}{(-\omega^2 m_s + j\omega c_s + k_s)(-\omega^2 m_{us} + k_t)}$$

2.2 Road Model

In early studies assessing vehicle dynamic performance, ground surface excitation in the form of deterministic shapes such as sine waves and step functions were often employed. Although these types of deterministic inputs could provide a basis for comparative evaluation of various suspension designs, they could not serve as a valid basis for evaluating the actual behaviours of the vehicle since the profile of the road surfaces are random functions.

Assuming that the random function of the road profiles are ergodic and stationary, the road profiles can be characterized by power spectral density (PSD) functions in the spatial domain. According to many previous studies, the relationship between the PSD and spatial frequency for road profiles can be sufficiently estimated by the following empirical model:

$$S(\Omega) = C_{sp}\Omega^{-n} \quad \textbf{(3.1)}$$

where,

S(Ω) is the PSD function of the road surface elevation

Ω is the spatial frequency, which is the inverse of wavelength

C_{sp} and n are constants

Over the years, there have been many attempts to classify the roughness of road surfaces based on the PSD function. Presently, the most well-known classification of road roughness is provided by the international organization for standardization (ISO 8608:1995), given in Table 2-1, in which the PSD function of ground surface profile is approximated by the following:

$$S(\Omega) = \begin{cases} S(\Omega_0)(\Omega/\Omega_0)^{-2} & if\ \ \Omega \leq 1/2\pi \\ S(\Omega_0)(\Omega/\Omega_0)^{-1.5} & if\ \ \Omega > 1/2\pi \end{cases} \quad \textbf{(3.2)}$$

where,

Ω is the spatial frequency expressed in cycles/m

Ω_o is the reference spatial frequency, $1/2\pi$ cycles/m,

$S(\Omega_o)$ is the degree of road roughness, given in Table 2-1.

Table 2-1 – ISO 8608:1995 Road Roughness Classification

Road Class	Degree of Roughness $S(\Omega_0)$, $10^{-6}m^2/cycles/m$	
	Range	Geometric Mean
A (Very good)	<8	4
B (Good)	8-32	16
C (Average)	32-128	64
D (Poor)	128-512	256
E (Very Poor)	512-2048	1024
F	2048-8192	4096
G	8192-32768	4096
H	>32768	16384

Figure 2-3 shows the PSD for road class A, B, and C (i.e. very good, good, and average) with respect to spatial frequency.

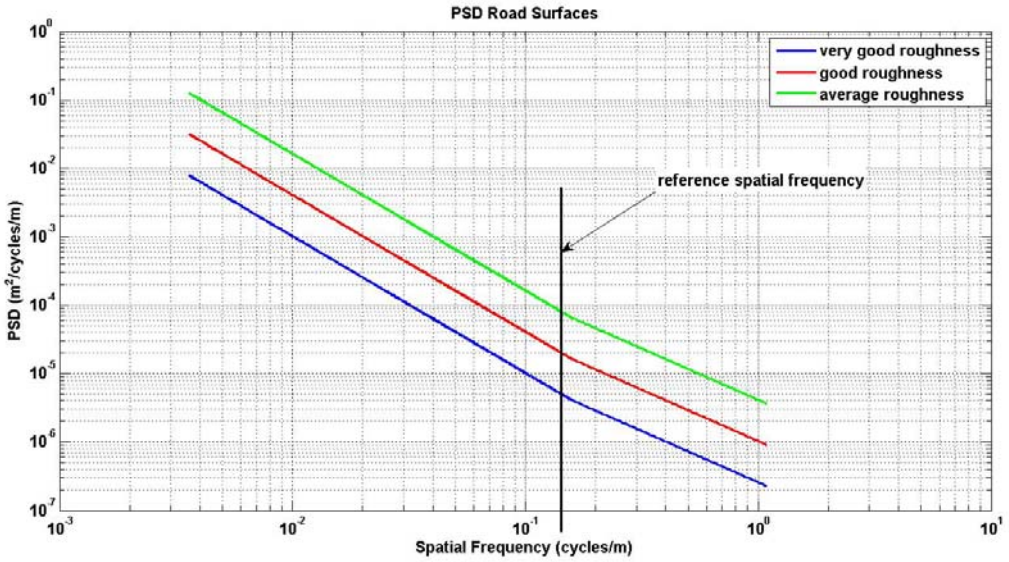

Figure 2-3: PSD function of ISO Road Surfaces

For on-road studies, road class A, B, C and D are generally employed as the means for exciting the quarter car model. Although the PSD road profile is expressed in terms of spatial frequency, for vehicle dynamic analysis using FRFs it is more convenient to express the PSD road profile in terms of temporal frequency, Hz, since vehicle vibration is a function of time. The relationship between spatial frequency and temporal frequency is as follows:

$$f = \Omega V \quad \textbf{(3.3)}$$

where,

f is the frequency in Hz

Ω is the spatial frequency expressed in cycles/m

V is the vehicle speed expressed in m/s

Using the above relationship, the transformation of the PSD road profile in terms of spatial frequency to one in terms of temporal frequency by means of the vehicle speed is expressed by the following relationship:

$$S(f) = \frac{S(\Omega)}{V} \quad \textbf{(3.4)}$$

where,

S(Ω) is the PSD function of the road surface elevation in spatial frequency

S(f) is the PSD function of the road surface elevation in temporal frequency

V is the vehicle speed expressed in m/s

2.2.1 **Road Profile Reconstruction**

For vehicle dynamic performance studies using the equations of motion, it is necessary to reconstruct the spectral function into a physical road profile. Converting the PSD function, representing specific road profile, into a height/distance relationship results in the following equations.

$$z_0(x) = \sum_{k=1}^{s} S_k sin(2\pi k \Delta\Omega x + \theta_k) \quad \textbf{(3.5)}$$

and

$$S_k = \sqrt{2(\Delta\Omega)S(k\Delta\Omega)} \quad \textbf{(3.6)}$$

where,

S_k are the amplitudes of the excitation harmonics evaluated from PSD function

$\Delta\Omega$ is the spatial frequency width considered

θ_k is the random phase angle

Figure 2-4 shows the reconstructed road elevations for road class A, B, and C (i.e. very good, good, and average) with respect to horizontal distance.

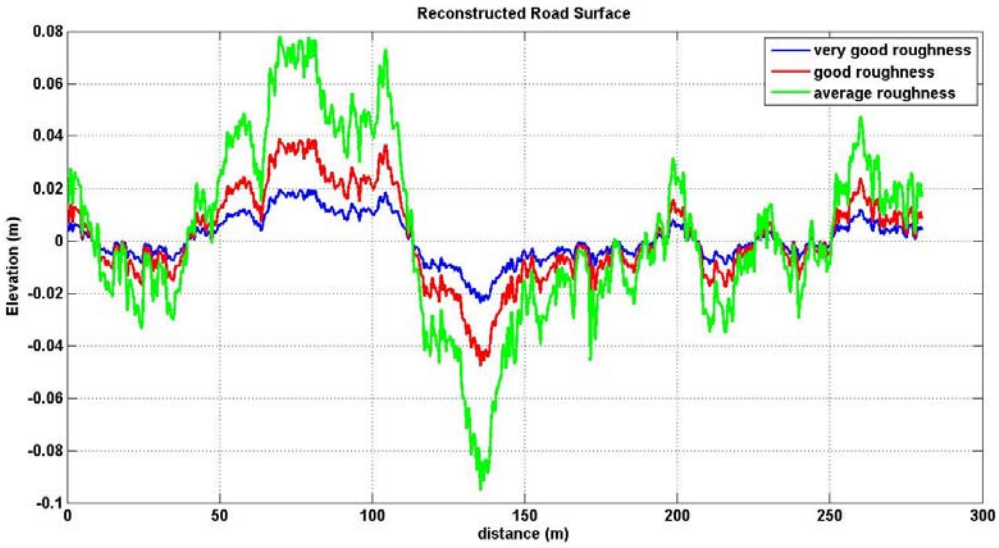

Figure 2-4: Reconstruction of ISO Road Surfaces from PSD functions

To transform the height/distance road profile into height/time road profile for use with the equations of motion simply divide the distance by vehicle speed.

Chapter 3

Semi-Active Controller Design

Recall that to enhance vehicle dynamic performance, using the added functionality from active elements, requires a controller to manage the element's properties. Since the tunable stiffness of the pneumatic spring is a slow acting element in comparison to the variable damper, traditional control algorithms employed for semi-active suspension would not be beneficial for this implementation. Most semi-active suspension systems regulate the damping property of the suspension system with the assumption that the damping property can be modified very quickly (i.e. high bandwidth element), which is not the case with the pneumatic spring design. The lag between the demanded stiffness and response of the pneumatic spring would cause undesirable vehicle responses. To leverage the advantage of the pneumatic spring, in conjunction with a variable damper, a lookup table control logic is employed to manage the stiffness and damping properties for enhancing the vehicle dynamic performance through various operating conditions. Since the road conditions and vehicle speed do not fluctuate frequently, the lookup table control logic has the ability to manage the low bandwidth pneumatic spring element without the constant fluctuation in demanded stiffness constant.

3.1 Lookup Table Controller Logic Structure

Lookup table control logic operates by performing predetermined actions, which in this instance is to manage the stiffness and damping property, based on specific operating conditions. Since the aim of this thesis is to develop a controller that adapts the suspension properties to varying sprung mass and road profile states, it is only natural for the sprung mass and road profile variations to define the operating conditions for this lookup table control logic. For this thesis, the sprung mass for the quarter car model ranges from 454.5 kg to 545.5 kg (i.e. 1000 lbs to 1200 lbs) to represent an average SUV vehicle [22]. Values of the road profile spans the on-road roughness from 0 to 512 x 10^{-6} m^2/cycles/m, as shown in Table 2-1, at 100km/h vehicle speed. Vehicle speed is set at 100km/h, the typical maximum legal vehicle speed limit in North American, because it generates the most severe

road profile when compared to lower vehicle speeds, which is depicted by the example temporal PSD curves in Figure 3-1. Hence, the vehicle at 100 km/h is the design envelop of the road profile definition. Vehicle speeds less than 100km/h would be classified using an equivalent road profile defined above.

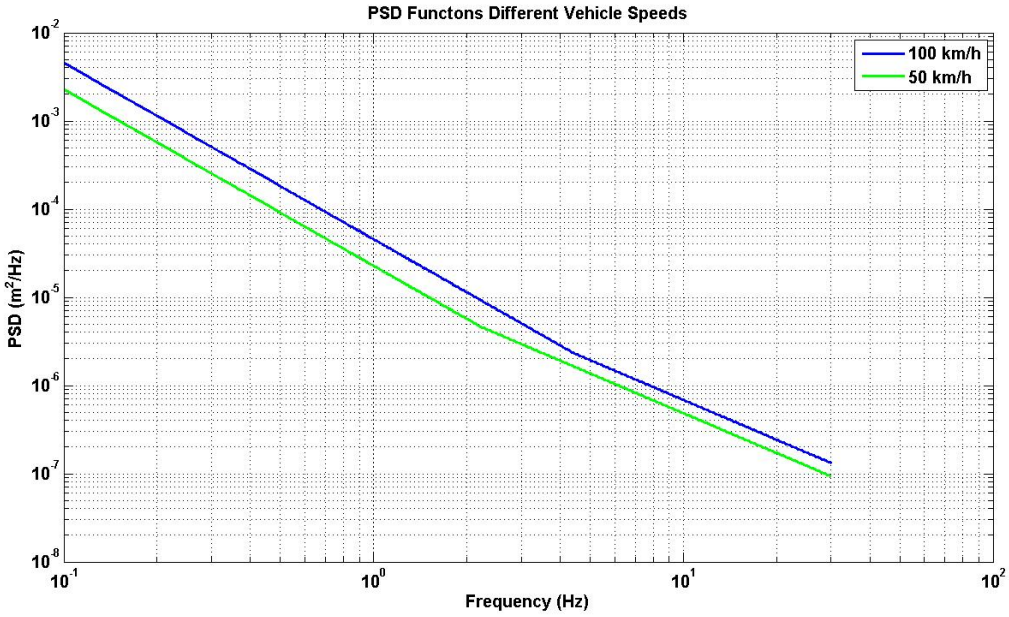

Figure 3-1: Comparison of Average Roughness PSD functions at different Vehicle Speeds

However, the range of sprung mass and road profile values, mentioned above, cannot directly define the operating conditions for the lookup table control logic, because of its continuous nature. As previously mentioned, the lookup table control logic uses specific operating conditions to drive predetermined actions, thus the continuous range of sprung mass and road profile values must be discretized. For this control logic, twelve operating conditions are proposed to cover the range of sprung mass and road profile values. The elements of the operating conditions comprise of the maximum, minimum, and mean value of the sprung mass range, and by four sets of the road profile, specified by the roughness range for on-road class A, B, C, and D in Table 2-1. The proposed structure of the control logic used for regulating the stiffness and damping properties (i.e. states) is shown in Figure 3-2.

Lookup Table Control Logic	
Operating Conditions	Actions
'Road Profile A' & '454.5 kg'	State 1
'Road Profile A' & '504.5 kg'	State 2
'Road Profile A' & '554.5 kg'	State 3
'Road Profile B' & '454.5 kg'	State 4
'Road Profile B' & '504.5 kg'	State 5
'Road Profile B' & '554.5 kg'	State 6
'Road Profile C' & '454.5 kg'	State 7
'Road Profile C' & '504.5 kg'	State 8
'Road Profile C' & '554.5 kg'	State 9
'Road Profile D' & '454.5 kg'	State 10
'Road Profile D' & '504.5 kg'	State 11
'Road Profile D' & '554.5 kg'	State 12

Figure 3-2: Proposed Lookup Table Control Logic Structure

Although the above controller logic appears to be a simple approach for the regulation of the stiffness and damping properties, this approach should enhance the vehicle dynamics performance. From the aforementioned studies, passive suspension systems yield desirable improvements in vehicle dynamic performance by tuning their stiffness and damping properties for specific operating conditions (i.e. sprung mass and road profile). However, vehicle dynamic performance for passive suspension systems can degrade due to deviations from their operating condition. By defining the actions of the lookup table control logic to be tuned stiffness and damping properties for a range of operating conditions, enhanced vehicle dynamics performance can be achieved under a wide range of operating conditions. To determine these tuned suspension parameters for each lookup table control logic operating condition, off-line optimization is employed due to the conflicting metrics in quantifying vehicle dynamics performance as illustrated in a topological flow diagram in Appendix A. The following section clarifies these conflicting metrics and the rationalization for employing optimization.

3.2 Optimization of Stiffness and Damping Properties

The primary goal of optimization is to find values within a design space that either maximizes or minimizes specified objective function(s). Hence, defining suitable objective functions and the range of the design space are essential for constructing the optimization problem and for ensuring appropriate optimal solution(s) are derived.

With respect to the control logic of the lookup table, there are twelve operating conditions stated which signifies twelve optimization problems are required to determine optimal values for the twelve operating conditions. To find these optimal solutions about each operating condition of the lookup table control logic, genetic algorithm (GA) is utilized since the algorithm has been used quite frequently in the optimization for passive suspension systems [10, 11, 18]. General workflow process of the GA algorithm is shown in Figure 3-3.

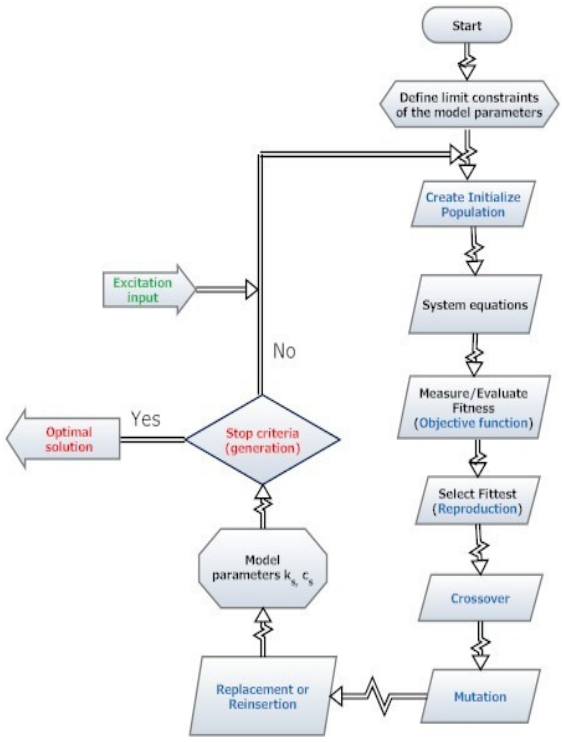

Figure 3-3: Schematic of a Generic Genetic Algorithm Workflow *[18]*

3.2.1 **Optimization Design Space**

The design space for this optimization is composed of two design variables, stiffness and damping. The range of values for the stiffness and damping properties are specified from the suspension design or requirement. In this case, the available range of stiffness and damping is derived from a proposed suspension design for a SUV vehicle. The following are the maximum and minimum stiffness and damping properties specified per the proposed suspension design:

k_s = {17600,…, 35200} N/m

c_s = {1500,…, 4500} Ns/m

3.2.2 **Objective Functions**

Since the aim of this thesis is to enhance the vehicle dynamic performance, the objective functions are the frequently used metrics used to quantify the vehicle dynamic performance objectively. For the quarter car model employed, there are four objective functions that are used to quantify the vehicle dynamic performance.

The first objective function quantify ride comfort of the vehicle by means of the weighted/filtered root mean square (RMS) value of the sprung mass acceleration response, as shown by the following relationship:

$$Obj1 = \begin{cases} \sqrt{\frac{1}{T}\int_0^T (\ddot{x}_{ws})^2 \, dt} & Time\ Domain \\ \quad or & \\ \sqrt{\sum_i (W_i a_i)^2} & Freq.\ Domain \end{cases} \qquad \textbf{(3.1)}$$

where,

$\ddot{x}_{ws}$ is the ISO filter sprung mass acceleration response

T is the time duration

i is the number of centre frequencies

W_i is the ISO weighting factor for ith octave band

a_i is the RMS sprung mass acceleration for ith octave band

Using the following relationship:

$$S_a(f) = |G_a(f)|^2 S_g(f)$$

where,

$S_a(f)$ is the acceleration PSD response

$G_a(f)$ is the acceleration FRF of the sprung mass

$S_g(f)$ is the ISO road PSD function

the RMS sprung mass acceleration, a_i, for the ith octave band is

$$\sqrt{\int_{0.89f_c}^{1.12f_c} S_a(f)\, df}$$

where,

f_c is the ISO specified centre frequencies

In Equation (3.1), the intent of the weighting factor/filter is to capture, objectively, the human response with respect to comfort per ISO 2631-1:1997. The values of the weighing factors and filter transfer function, as defined in ISO 2631-1:1997, are shown in Appendix B.

The second and third objective functions quantify the rattle space and handling performance by means of the RMS value for suspension deflection and tire deflection response, respectively. The expression for the RMS suspension deflection and RMS tire deflection are as follows:

$$Obj2 = \begin{cases} \sqrt{\frac{1}{T}\int_0^T z\, dt} & Time\ Domain \\ \quad or & \\ \sqrt{\int_{f1}^{f2} S_z(f)} & Frequency\ Domain \end{cases} \qquad \textbf{(3.2)}$$

where,

z is the suspension deflection response

T is the time duration

$f1$ and $f2$ are boundary frequencies of the interval

$S_z(f) = |H(f) \times G(f)|^2 S_g(f)$ is the suspension deflection PSD response, $H(f)$ is the suspension deflection FRF, $G(f)$ is the unsprung deflection FRF, and $S_g(f)$ is the ISO road PSD function

$$Obj3 = \begin{cases} \sqrt{\frac{1}{T}\int_0^T y\, dt} & Time\ Domain \\ \quad or & \\ \sqrt{\int_{f1}^{f2} S_y(f)} & Frequency\ Domain \end{cases} \quad \textbf{(3.3)}$$

where,

y is the tire deflection response

T is the time duration

$f1$ and $f2$ are boundary frequencies of the interval

$S_y(f) = |H(f)|^2 S_g(f)$ is the tire deflection PSD response, $H(f)$ is the tire deflection FRF, and $S_g(f)$ is the ISO road PSD function

For convenience, Equations (3.1) to (3.3) expresses the RMS formulations in both time domain and frequency domain to accommodate the developed quarter car model, which can be expressed by either the equations of motions or frequency response functions. Note that the RMS formulations are functions of the sprung mass and road profile, which are the components of the control logic operating conditions.

The last objective function captures the undamped sprung mass natural frequency quantity by finding the eigenvalues in Equation (2.7). Note that this objective function is a function of only one component of the control logic operating conditions, which is the sprung mass.

In terms of improving vehicle dynamic performance, it is desirable to minimize the ride comfort, rattle space and handling RMS values while maximizing the undamped sprung mass natural frequency value. Minimizing the RMS values reduces ride discomfort, and reduces the suspension and tire deflection variation, respectively, while maximizing the undamped sprung mass natural

frequency value enforces the natural frequency above 1Hz to avoid passenger motion sickness [21]. Passenger motion sickness is most predominant when the undamped sprung mass natural frequency is below 1Hz. If the objective functions maximum and minimum occurred synchronously within the design space, the optimal solution for the stiffness and damping properties of a suspension system would be trivial. However, the maximum and minimum values of the objective functions occur at different values within the design space, thus finding an optimal solution is non-trivial. Shown in Table 3-1 are the design values at each objective function's maximum and minimum, as determined by GA.

Table 3-1 – Design Values for Objective Function Maximum and Minimum Values

Objective Functions	454.5 kg Design Values (k_s & c_s)	504.5 kg Design Values (k_s & c_s)	554.5 kg Design Values (k_s & c_s)
RMS Ride Comfort Maximum	35200 kN/m, 4500 Ns/m	35200 kN/m, 4500 Ns/m	35200 kN/m, 4500 Ns/m
RMS Ride Comfort Minimum	17600 kN/m, 1500 Ns/m	17600 kN/m, 1500 Ns/m	17600 kN/m, 1500 Ns/m
RMS Suspension Deflection Maximum	17600 kN/m, 1500 Ns/m	17600 kN/m, 1500 Ns/m	17600 kN/m, 1500 Ns/m
RMS Suspension Deflection Minimum	35200 kN/m, 4500 Ns/m	35200 kN/m, 4500 Ns/m	35200 kN/m, 4500 Ns/m
RMS Tire Deflection Maximum	35200 kN/m, 1500 Ns/m	35200 kN/m, 1500 Ns/m	35200 kN/m, 1500 Ns/m
RMS Tire Deflection Minimum	17782.3 kN/m, 2850.1 Ns/m	17600 kN/m, 2894.4 Ns/m	17600 kN/m, 2933.4 Ns/m
Undamped m_s Natural Freq. Maximum	35200 kN/m, 4500 Ns/m	35200 kN/m, 4500 Ns/m	35200 kN/m, 4500 Ns/m
Undamped m_s Natural Freq. Minimum	17600 kN/m, 1500 Ns/m	17600 kN/m, 1500 Ns/m	17600 kN/m, 1500 Ns/m

Note that the design values for the maximum and minimum values of the objective function are insensitive to the varying operating conditions, with the exception of the minimum tire deflection, which is marginally sensitive to sprung mass variation. Due to this conflict between the occurrences of each objective function's maximum and minimum, optimization is employed to find the best design values.

3.2.3 **Normalization of Objective Functions**

To comprehend the objective function values relative to their achievable maximum and minimum values within the design space, the objective functions are normalized. The normalization of the objective functions, in this case, measures the distance between the objective function value and their achievable minimum value relative to the distance between their achievable maximum and minimum, as shown by the following equations:

$$Obj1_{norm} = \frac{Obj1 - Obj1_{min}}{Obj1_{max} - Obj1_{min}} \quad \textbf{(3.4)}$$

$$Obj2_{norm} = \frac{Obj2 - Obj2_{min}}{Obj2_{max} - Obj2_{min}} \quad \textbf{(3.5)}$$

$$Obj3_{norm} = \frac{Obj3 - Obj3_{min}}{Obj3_{max} - Obj3_{min}} \quad \textbf{(3.6)}$$

$$Obj4_{norm} = \frac{Obj4 - Obj4_{min}}{Obj4_{max} - Obj4_{min}} \quad \textbf{(3.7)}$$

Thus, from Equation (3.4) to (3.7), when the normalized objective function equals zero the objective functions are at its minimum value, and when the normalized objective functions equals one, the objective function is at its maximum.

3.2.4 **Multiobjective Optimization Methodology**

With the above normalized objective functions established, there are two multiobjective optimization approaches available to determine the optimal design solution(s). The first approach is to create a weighted linear sum of the objective functions called a single aggregate objective function, which produces a single optimal design solution. This approach is not employed for these optimization problems because the added weighting factors introduce subjectivity and *a priori* knowledge to the optimized solution.

The second approach optimizes the objective functions concurrently to generate a set of design solutions called the Pareto optima set. Recall that the design values from a Pareto optima set are called non-dominated solutions since there are no design values that can improve an objective function's value without degrading the other objective functions values. This approach is favoured over the optimization of the single aggregate objective function because the Pareto optima set provides all the solution candidates, which allows for more objectivity and trade-off studies to be performed when selecting particular solutions from the Pareto optima set.

3.2.5 **Pareto Optima Results**

For these optimization problems, the quarter car model fixed parameters (i.e unsprung mass and tire stiffness), which represent a typical SUV vehicle [22], are as follows:

m_{us} = 45.45 kg

k_t = 170 kN/m

The frequency domain RMS objective functions are used for optimization as their algebraic formulation permits the direct determination of the objective functions values. The frequency bandwidth, to calculate the RMS objective functions, is from 0.05Hz to 30Hz. Road-induced vibrations are typically below 30 Hz, and have an amplitude greater than 0.3 mm [19]. Optimization of the objective functions are about the geometric mean of on-road profile A, B, C, and D in Table 2-1.

Since the quarter car model is linear time-invariant (LTI), the road profile PSDs, at 100km/h, are linear scales of one another as illustrated in Figure 3-4, and the objective functions are normalized, the number of optimization problems can be reduced significantly. The reason for this significant reduction is because the above linear traits generate equivalent Pareto values regardless of road profile. Thus, only one road profile is needed to determine the Pareto optima sets, which, in turn, reduces the number of optimization problems from twelve, which is the number of operating conditions defined, to three.

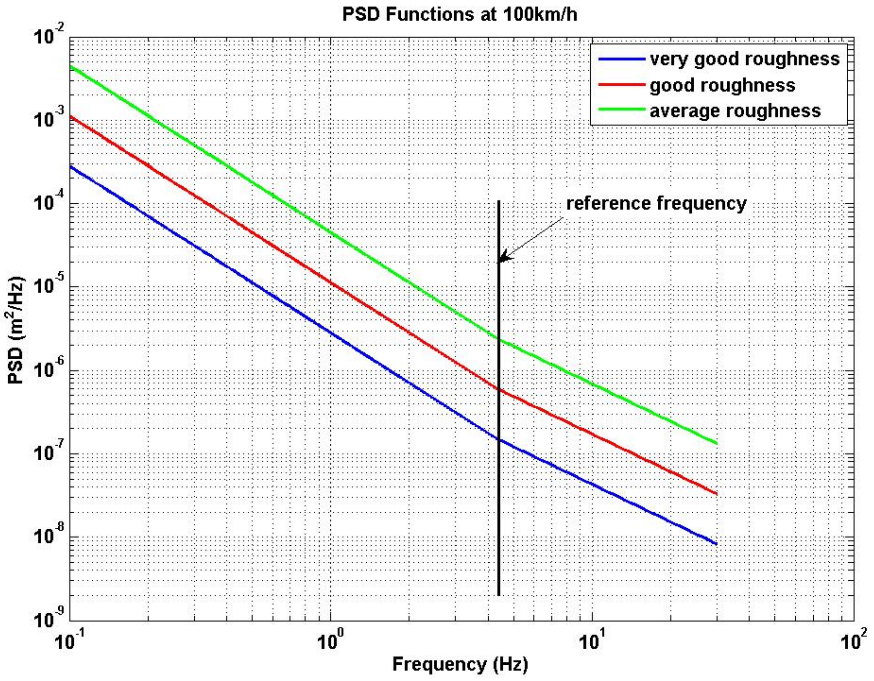

Figure 3-4: Comparison of PSD Functions for different road roughness at 100km/h

The Pareto surface of the objective function values, excluding the sprung natural frequency values, for each of the three sprung mass value, are presented in Figure 3-5 to Figure 3-7.

Comparing the Pareto surface above by overlaying their respective surfaces reveals that the objective functions RMS values relatively converge when the handling RMS value (i.e. tire deflection) is below approximately 0.3. Within this convergence region the normalized objective functions values for each sprung mass are approximately within +/- 2% of each other when using the same design values. Figure 3-8 illustrates the region of convergence from the overlay of Pareto surfaces. Therefore, when the handling RMS value is below approximately 0.3, the design solutions and their respective objective function values are generally mass invariant.

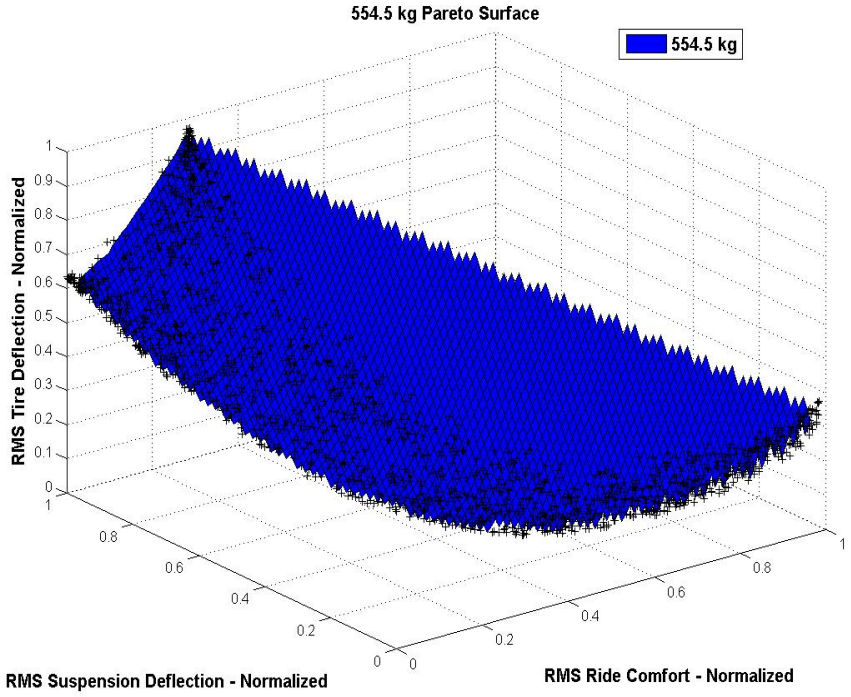

Figure 3-5: Pareto Surface for 554.5kg Sprung Mass

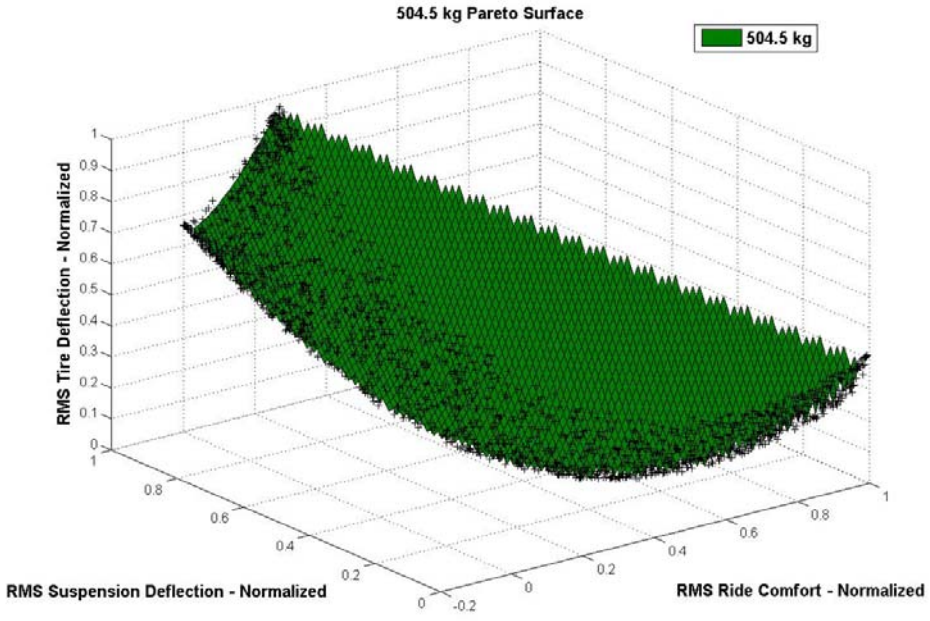

Figure 3-6: Pareto Surface for 504.5kg Sprung Mass

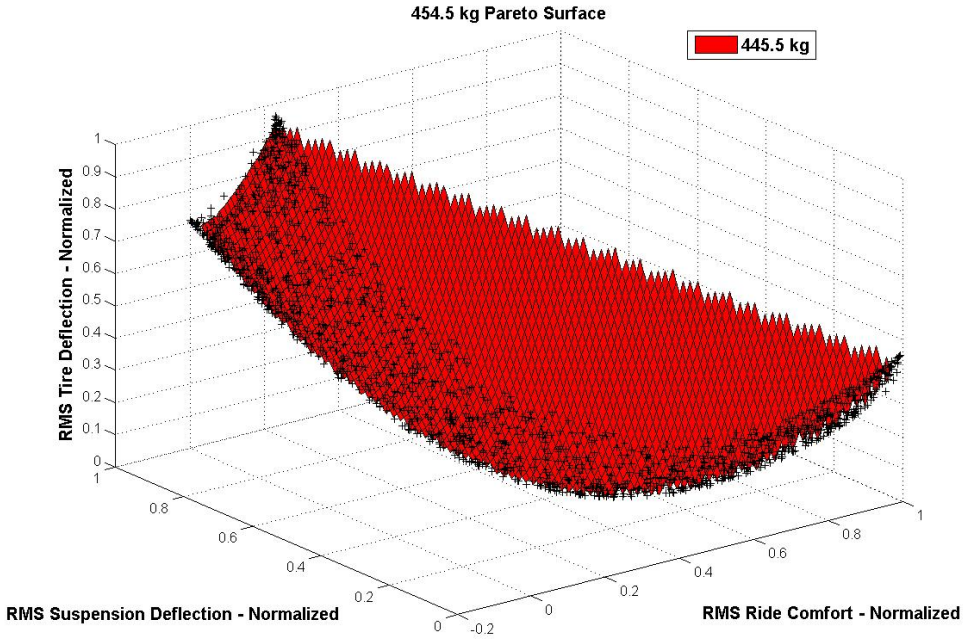

Figure 3-7: Pareto Surface for 454.5kg Sprung Mass

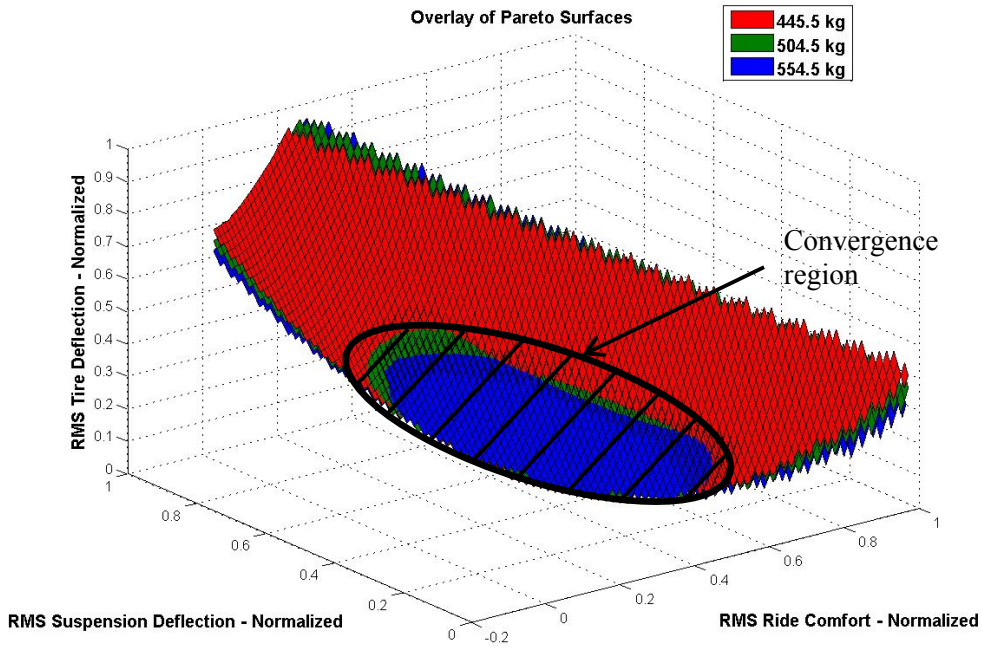

Figure 3-8: Convergence Region from Overlay of Pareto Surfaces

3.2.6 **Trade-Off Study and Selected Solutions**

To begin the trade-off study, the criteria for selecting a solution from the Pareto optima set for road profile A and D, which have the smallest and largest road roughness, are founded first. For the case when road profile A is considered, the desire is to maximize sprung mass RMS acceleration and sprung mass natural frequency value, and minimize the rattle space RMS regardless of the sprung mass quantity. These criteria are founded because it is desirable, under very good road condition, to sacrifice the ride comfort and handling performance, which are extremely small RMS values in this instance, for the allowance of the best rattle space performance and for maximizing undamped sprung mass natural frequency above 1Hz. The sprung mass condition is ignored in this regime because the general RMS values and variations are small relative to other road profiles and do not impact vehicle dynamics performance greatly.

When road profile D is considered for each sprung mass condition, the desires to minimize the sprung mass RMS acceleration and tire RMS deflection values takes precedence over the minimization of rattle space RMS and maximization of the undamped sprung mass natural frequency values. The reason why minimizing sprung mass RMS acceleration and handling takes precedence is because the RMS values for sprung mass acceleration and handling are large when traversing road profile D and would adversely affect passenger comfort which leads to poor vehicle performance. Thus, compromises are made in rattle space performance and undamped sprung mass natural frequency to achieve minimized sprung mass RMS acceleration and handling. In terms of rattle space performance constraint, the maximum RMS suspension deflection allowable, assuming Gaussian distribution and zero mean, is 0.03 m (i.e. three standard deviations) to accommodate a rattle space of 0.1 m.

With the criteria for the smallest and largest road roughness finalized, the criteria for road profile C and D are established. The criteria for road profile C and D should be a trade-off between the finalized criteria for road profile A and D. With respect to road profile C for each sprung mass condition, the road comfort performance and sprung mass natural frequency should be biased towards their maximum values, while the rattle space performance should be biased towards the minimum. Conversely, with respect to road profile D for each sprung mass condition, the road comfort performance and sprung mass natural frequency should be biased towards their minimum values,

while the rattle space performance should be biased towards the maximum. In both cases, the handling performance is to be minimized within their respective trade-off space defined. In Table 3-2, are the selection criteria for the trade-off study with respect to each road profile.

Table 3-2 – Selection Criteria for Design Values per Operating Conditions

Operating Conditions	Normalized RMS Sprung Mass Acceleration	Normalized RMS Suspension Deflection	Normalized RMS Tire Deflection	Normalized Undamped m_s Natural Freq.
Road Profile D	min –in tandem	< 0.03m	min –in tandem	N/A
Road Profile C	~1/3 between (max and min)	~2/3 between (max and min)	Min	~1/3 between (max and min)
Road Profile B	~2/3 between (max and min)	~1/3 between (max and min)	Min	~2/3 between (max and min)
Road Profile A	max	Min	N/A	Max

The design values and normalized objective function values selected using the trade-off criteria above for the each sprung mass operating condition and road condition are presented in Table 3-3 to Table 3-5.

Table 3-3 – Design and Normalized Objective Function Values for 554.5 kg Sprung Mass

554.5 kg	k_s	c_s	RMS Sprung Mass Acceleration (m/s^2)	RMS Suspension Deflection (m)	RMS Tire Deflection (m)	Undamped m_s Natural Freq. (rad/s)
Road Profile D	18601.61	1995.06	0.21	0.69	0.21	0.07
Road Profile C	22521.58	2848.52	0.52	0.35	0.03	0.33
Road Profile B	28552.89	3339.79	0.69	0.22	0.11	0.68
Road Profile A	35141.27	4499.76	1.00	0.00	0.39	1.00

Table 3-4 – Design and Normalized Objective Function Values for 504.5 kg Sprung Mass

504.5kg	k_s	c_s	RMS Sprung Mass Acceleration (m/s^2)	RMS Suspension Deflection (m)	RMS Tire Deflection (m)	Undamped m_s Natural Freq. (rad/s)
Road Profile D	19022.53	2015.33	0.22	0.68	0.21	0.10
Road Profile C	22641.30	2847.17	0.52	0.35	0.02	0.34
Road Profile B	28475.96	3289.28	0.67	0.23	0.10	0.67
Road Profile A	34439.42	4470.28	1.00	0.00	0.42	1.00

Table 3-5 – Design and Normalized Objective Function Values for 454.5 kg Sprung Mass

454.5kg	k_s	c_s	RMS Ride Comfort	RMS Suspension Deflection	RMS Tire Deflection	Undamped m_s Natural Freq.
Road Profile D	19278.61	2022.43	0.22	0.67	0.20	0.12
Road Profile C	22619.91	2875.51	0.53	0.34	0.01	0.34
Road Profile B	29268.62	3310.53	0.68	0.23	0.10	0.71
Road Profile A	35200.00	4500.00	1.00	0.00	0.46	1.00

As shown in Table 3-3 to Table 3-5, the handling normalized value for road profile B, C, and D are below for 0.3 for each sprung mass operating condition. This reveals that a single set of design values from Table 3-3 to Table 3-5 can be considered for all sprung mass operating conditions because the values of the Pareto set converges when the handling normalized value is below 0.3. Thus, due to this convergence of Pareto values, the optimal design values can be considered mass invariant. This outcome significantly reduces the number of operating conditions, which are now solely based on the road conditions, and hence reduces the complexity of the lookup table control logic. The design values with the smallest handling normalized value among the three sprung mass conditions for road profile B, C, and D in Table 3-3 to Table 3-5 is selected as the design value for all sprung mass conditions. Table 3-6 summarizes the updated optimal design values, which are suitable across all sprung mass conditions, for each road condition.

Table 3-6 – Design Values for Lookup Table Controller

Road Profile	k_s	c_s
Road Profile D	19278.61	2022.43
Road Profile C	22619.91	2875.51
Road Profile B	28475.96	3289.28
Road Profile A	35200.00	4500.00

3.3 Implementation of Lookup Table Controller

To evaluate the performance of the lookup table control logic, the lookup table control logic is implemented into a MATLAB Simulink quarter car model, shown in Figure 3-10.

The control logic architecture of the lookup table is updated in Figure 3-9 to reflect that the sprung mass element within the operating conditions of the control logic are not required for determining the lookup table control logic actions. The states within the lookup table control logic are the design values (k_s and c_s) specified in Table 3-6.

Lookup Table Control Logic	
Operating Conditions	Actions
'Road Profile A'	State 4
'Road Profile B'	State 3
'Road Profile C'	State 2
'Road Profile D'	State 1

Figure 3-9: Updated Lookup Table Control Logic Structure

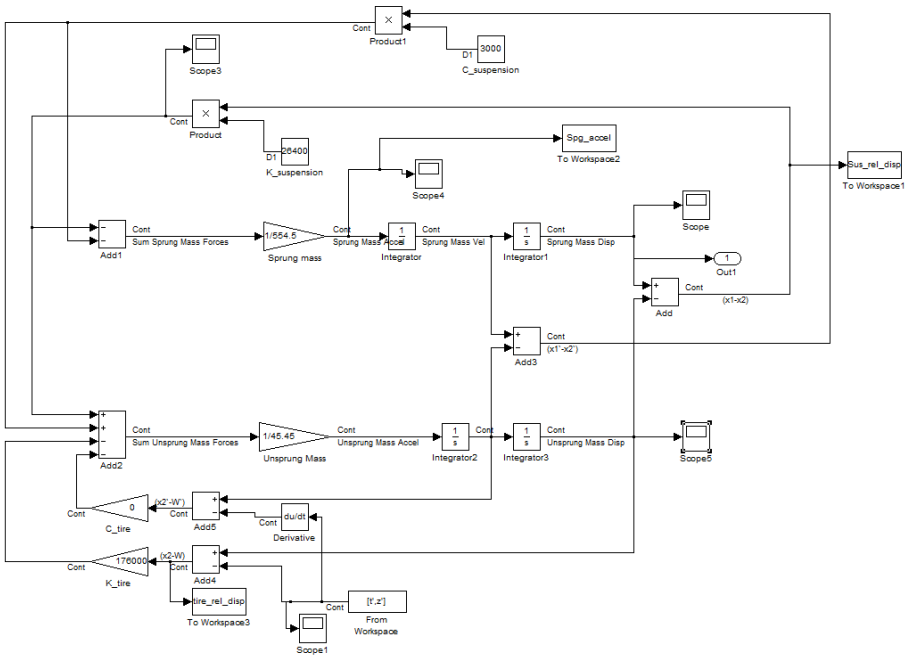

Figure 3-10: Schematic of MATLAB/Simulink Quarter Car Model

Although the control logic operating conditions uses the type of road conditions to dictate the actions, there is no direct method to recognize the type of road conditions that the vehicle would experience. It is purposed to identify the road condition type through indirect means by using the RMS value of the unsprung mass acceleration. To ensure that the RMS unsprung mass acceleration values are a reliable source for identifying the road conditions, the RMS value should be relatively insensitive to changes in sprung mass in order to accommodate the control logic specified operating conditions in Figure 3-9. The RMS value of the unsprung mass acceleration for the three different sprung mass using the selected design values for road profile A and B are shown in Table 3-7.

Table 3-7 – Comparison of Unsprung Mass RMS Acceleration between States and Sprung Mass

	454.5 kg & State 4 (m/s^2)	554.5 kg & State 4 (m/s^2)	554.5 kg & State 3 (m/s^2)
Road Profile D	12.48	12.49	15.30
Road Profile C	6.24	6.25	7.65
Road Profile B	3.12	3.12	3.83
Road Profile A	2.21	2.21	2.71

From Table 3-7, the RMS values differ by a maximum of approximately 1% across the sprung mass conditions and therefore are suitable for identifying road conditions. However, the RMS value of the unsprung mass acceleration, in Table 3-7, varies between the two selected design values. To overcome this drawback, the lookup table control logic incorporates the state of the stiffness and damping properties, in addition to the RMS unsprung mass acceleration value, as part of its operating conditions. Using the revised operating conditions above, the concluded lookup table control logic is presented in Figure 3-11. The RMS unsprung mass acceleration values for the transitions between road profile A and B, B and C, and C and D, per suspension property state are shown in Table 3-8.

Lookup Table Control Logic	
Operating Conditions	Actions
'Road Profile Transition A→B' & 'State 1'	State 2
'Road Profile Transition A→C' & 'State 1'	State 3
'Road Profile Transition A→D' & 'State 1'	State 4
'Road Profile Transition B→A' & 'State 2'	State 1
'Road Profile Transition B→C' & 'State 2'	State 3
'Road Profile Transition B→D' & 'State 2'	State 4
'Road Profile Transition C→A' & 'State 3'	State 1
'Road Profile Transition C→B' & 'State 3'	State 2
'Road Profile Transition C→D' & 'State 3'	State 4
'Road Profile Transition D→A' & 'State 4'	State 1
'Road Profile Transition D→B' & 'State 4'	State 2
'Road Profile Transition D→C' & 'State 4'	State 3

Figure 3-11: Proposed Lookup Table Control Logic Structure using RMS Unsprung Accelerations and Suspension States

Table 3-8 – Unsprung Mass RMS Acceleration at Road Profile Transitions

Road Profile Transition	State 1 m_{us} RMS Values (m/s^2)	State 2 m_{us} RMS Values (m/s^2)	State 3 m_{us} RMS Values (m/s^2)	State 4 m_{us} RMS Values (m/s^2)
Road Profile Transition C↔D	20.39	16.62	15.30	12.49
Road Profile Transition B↔C	10.20	8.31	7.65	6.25
Road Profile Transition A↔B	5.10	4.16	3.83	3.12

Although the overall lookup table control logic is complete, the implementation of the lookup table controller into the time-based Simulink quarter car model requires that the unsprung mass acceleration signal from the quarter car model be preprocessed. The preprocessing of the unsprung mass acceleration signal is required because the Simulink quarter car model outputs the unsprung mass acceleration response in real-time, which does not match the control logic use of RMS values of the for its operating conditions. Assuming that the unsprung mass acceleration signal has a Gaussian distribution with a mean of zero indicates statistically that the standard deviations of the signal are equivalent to RMS values of the control logic operating conditions. Using this statistical property provides the basis for adapting to the quarter car model with the lookup table controller. In Simulink, the unsprung mass acceleration signal is preprocessed, using moving windows of 10 seconds with sampling rates of 100Hz, to have their statistical properties examined. Using the fact that the standard deviation of unsprung mass acceleration signal is equal to the RMS transition values in Table 3-8, it is expected that 33 percent or less of the data points within a 10 second window would exceed the RMS transition values. When greater than 33 percent of the data points are above the RMS transition value, it is likely that the road profile conditions has switched and the suspension properties should change state accordingly. Through this method of preprocessing the unsprung mass acceleration signal, the lookup table controller can now operate within the Simulink quarter car model. This approach is adopted because it is simple and does not require calculation of the road prolife RMS or estimation of the road profile frequency content.

An inherent drawback using lookup table control logic, that is well known, is the flip-flop effect when the operating conditions are about the transition between two neighbouring operating conditions of

the control logic. To alleviate the inherent drawback of using lookup table control logic, a temporal deadband is utilized. The temporal deadband implemented for this control logic compares the statistical properties of the moving windows for a span of 5 seconds to ensure the likelihood of transitioning from one suspension state to the neighbouring. If the statistical property of the 10 seconds moving window remains unchanged within the deadband, the likelihood is that the operating conditions have changed and the current suspension state should be updated to the neighbouring suspension state, otherwise the current suspension state should remain unchanged. The MATLAB code used within Simulink for signal preprocessing, control logic, and temporal deadband can be found in Appendix C.

Chapter 4

Vehicle Dynamic Performance Results

To evaluate the vehicle performance of the semi-active suspension using the combination of pneumatic spring and variable damper and the controller developed in this thesis, a passive suspension system is used as a baseline comparison. The results presented within this chapter are outlined as follows:

- Time history and controller response
- Vehicle performance results and comparison
- Summary

Results were generated using a Simulink quarter car passive model and Simulink quarter car model with the lookup table controller. Figure 4-1 and Figure 4-2 are the Simulink models used for evaluating vehicle performance.

The fixed MATLAB/Simulink parameters used for evaluating vehicle performance are equivalent to the parameters used to produce the Pareto optima set. To recap, the parameters are as follows:

m_{us} = 45.45 kg

k_t = 170 kN/m

The passive suspension properties for the baseline model are:

k_s = 26.4 kN/m

c_s = 3 kN·s/m

These values are the median points in the design space. Selection of these parameters values for establishing the baseline are due to the compromise between a very soft and stiff suspension system that can be achieved with the pneumatics spring and variable damper.

Lastly, the vehicle performance is evaluated at the following sprung mass values:

m_s = 454.5 kg , 504.5 kg, 554.5 kg

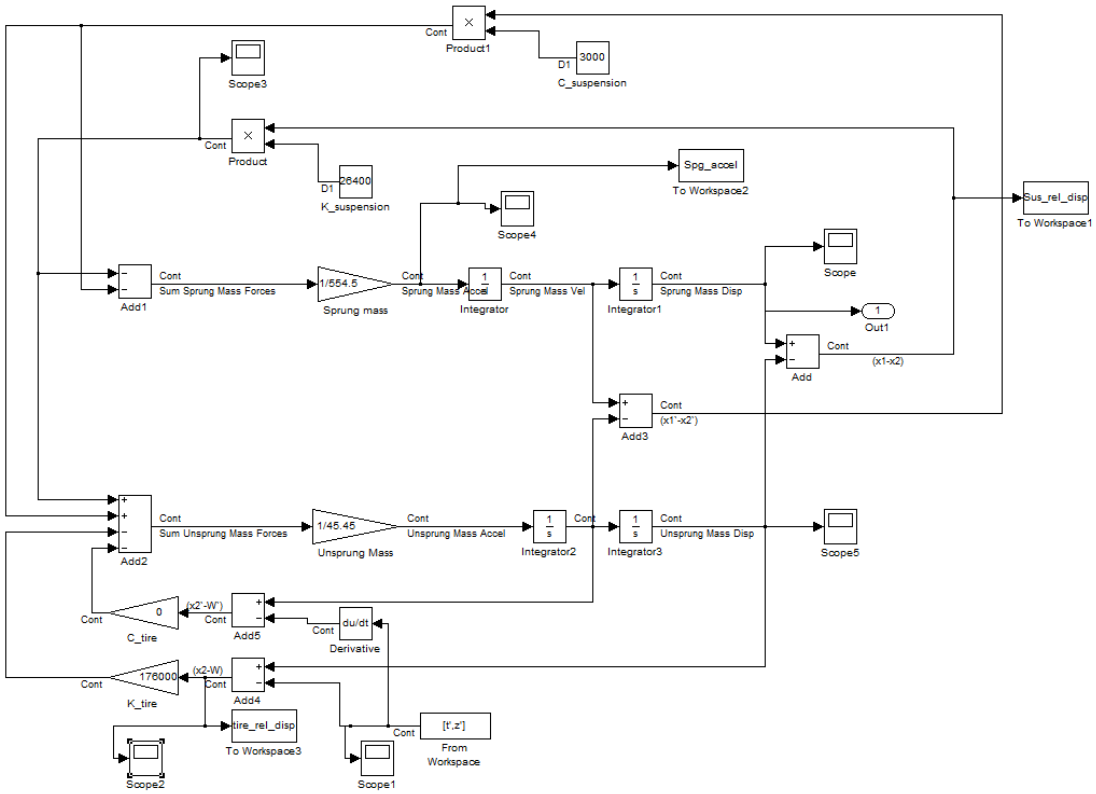

Figure 4-1: Schematic of MATLAB/Simulink Passive Quarter Car Model

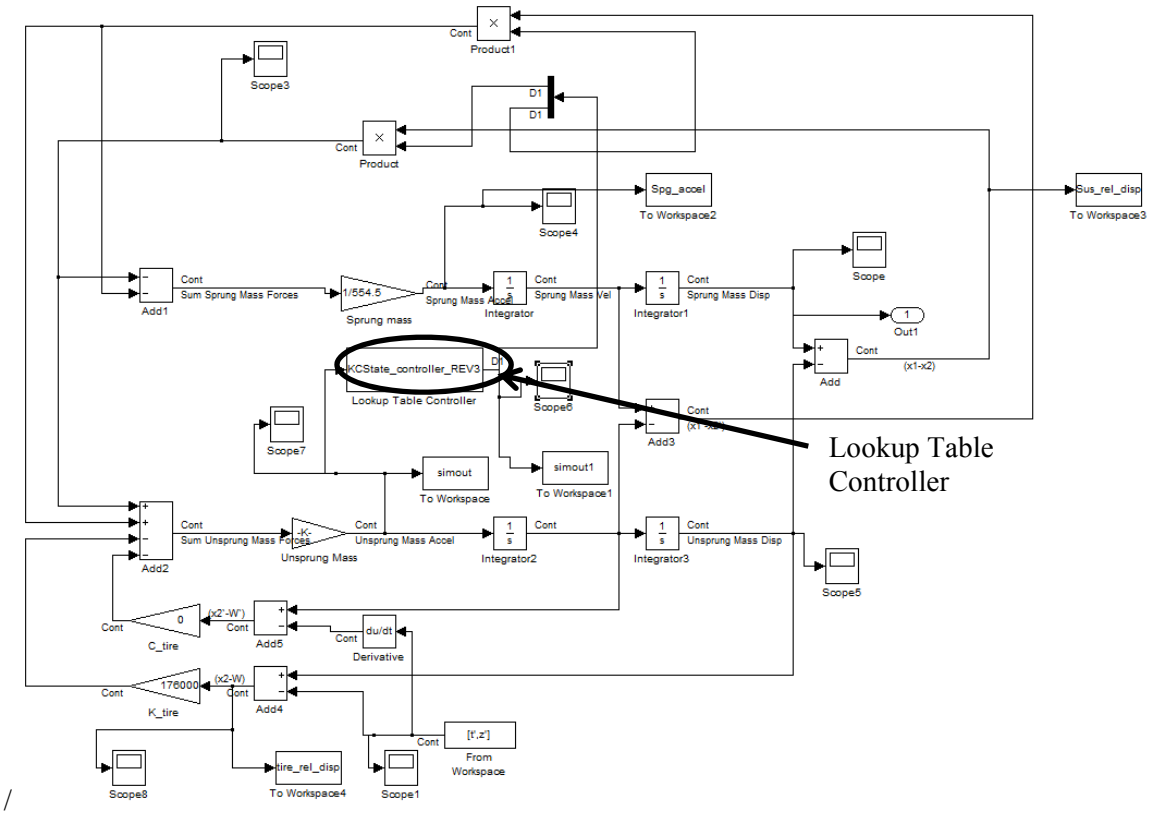

Figure 4-2: Schematic of MATLAB/Simulink Quarter Car Model with Lookup Table Controller

Road courses used to for evaluation purpose are as follows in Table 4-1 to Table 4-3.

Table 4-1 – Road Course 1 to evaluate Lookup Table Controller versus Road Roughness

Road Course 1	
Road Roughness Number	Vehicle Speed
4 x $10^{-6} m^2/cycles/m$	100 km/h
256 x $10^{-6} m^2/cycles/m$	100 km/h

Table 4-2 – Road Course 2 to evaluate Lookup Table Controller versus Vehicle Speed

Road Course 2	
Road Roughness Number	Vehicle Speed
45 x $10^{-6}m^2/cycles/m$	100 km/h
45 x $10^{-6}m^2/cycles/m$	60 km/h

Table 4-3 – Road Course 3 to evaluate Lookup Table Controller between Neighbouring States

Road Course 3	
Road Roughness Number	Vehicle Speed
140 x $10^{-6}m^2/cycles/m$	100 km/h
120 x $10^{-6}m^2/cycles/m$	100 km/h

These three road courses are used to evaluate the different facets of the lookup table controller. Road course 1 is used to evaluate the lookup table controller overall detection ability and performance. Road courses 2 and 3 are used to evaluate the lookup table controller over different vehicle speeds and between neighbouring states, respectively. The reconstruction of the above road courses from their respective PSD functions are shown in Appendix D.

4.1 Time History and Controller Response

Figure 4-3 to Figure 4-11 are the sprung mass acceleration, unsprung mass acceleration, suspension deflection, tire deflection, controller response per each road course at 454.5, 504.5, and 554.5 kg sprung mass.

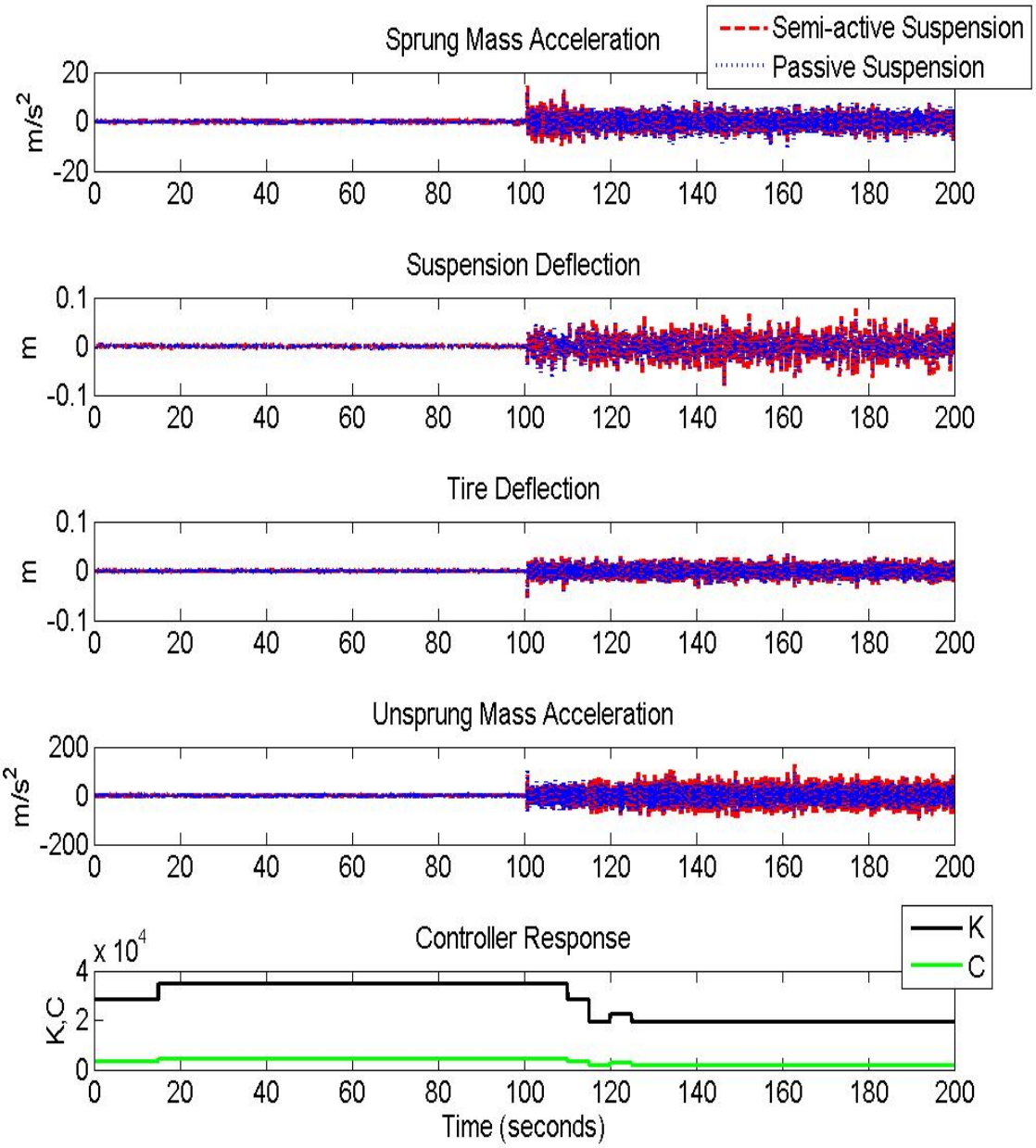

Figure 4-3: Time History and Controller Response at 454.5 kg Sprung Mass traversing Road Course 1

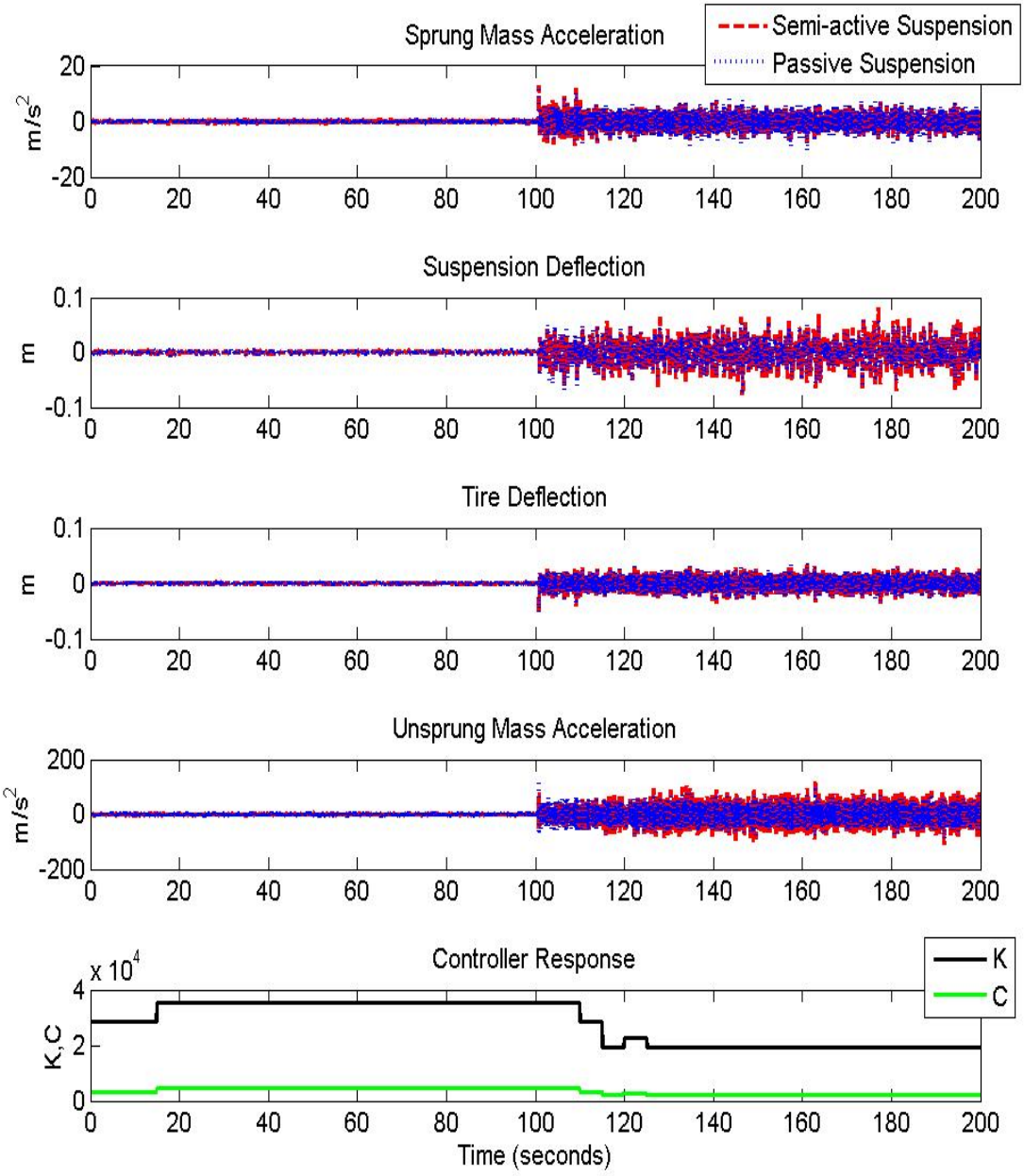

Figure 4-4: Time History and Controller Response at 504.5 kg Sprung Mass traversing Road Course 1

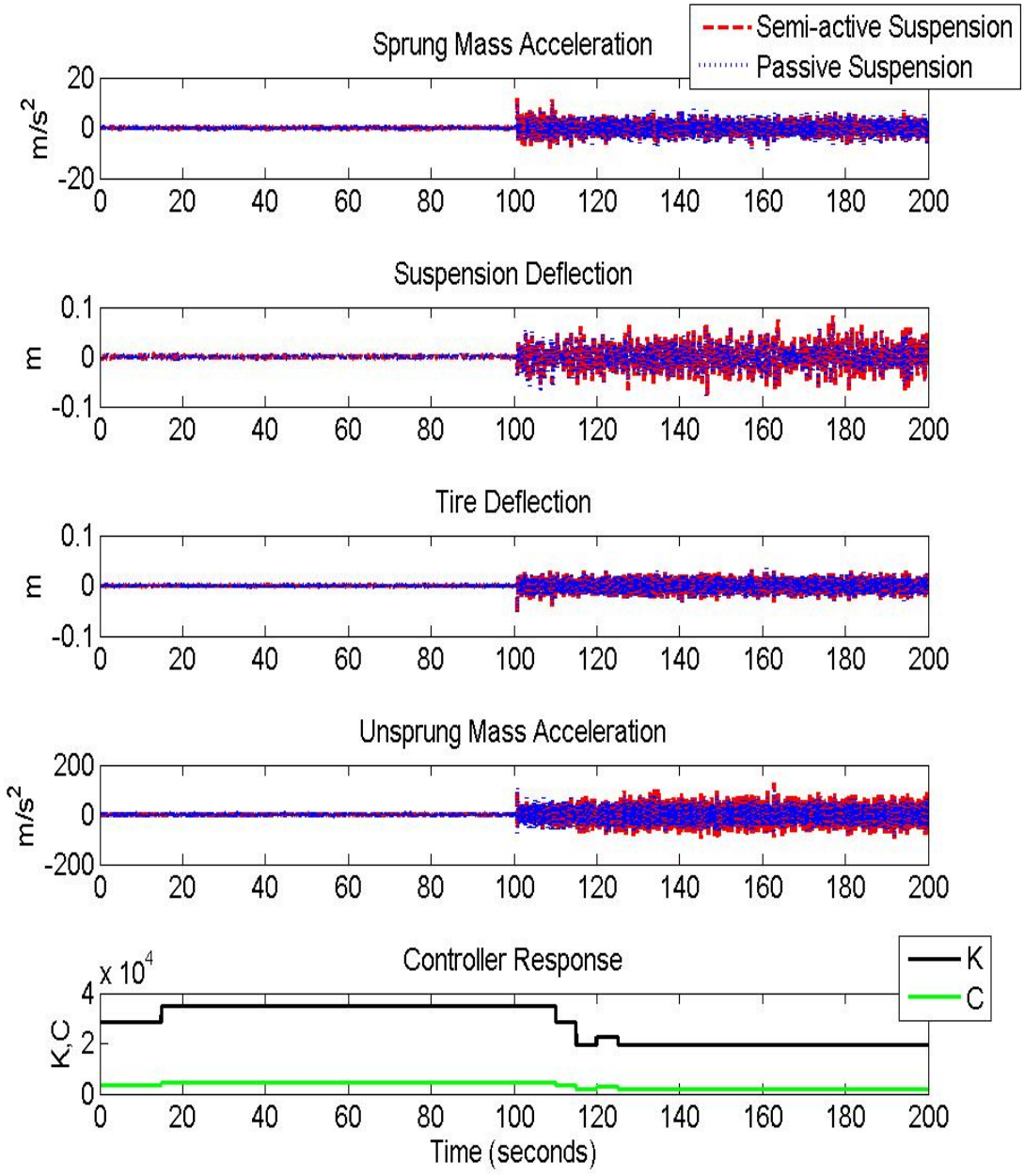

Figure 4-5: Time History and Controller Response at 554.5 kg Sprung Mass traversing Road Course 1

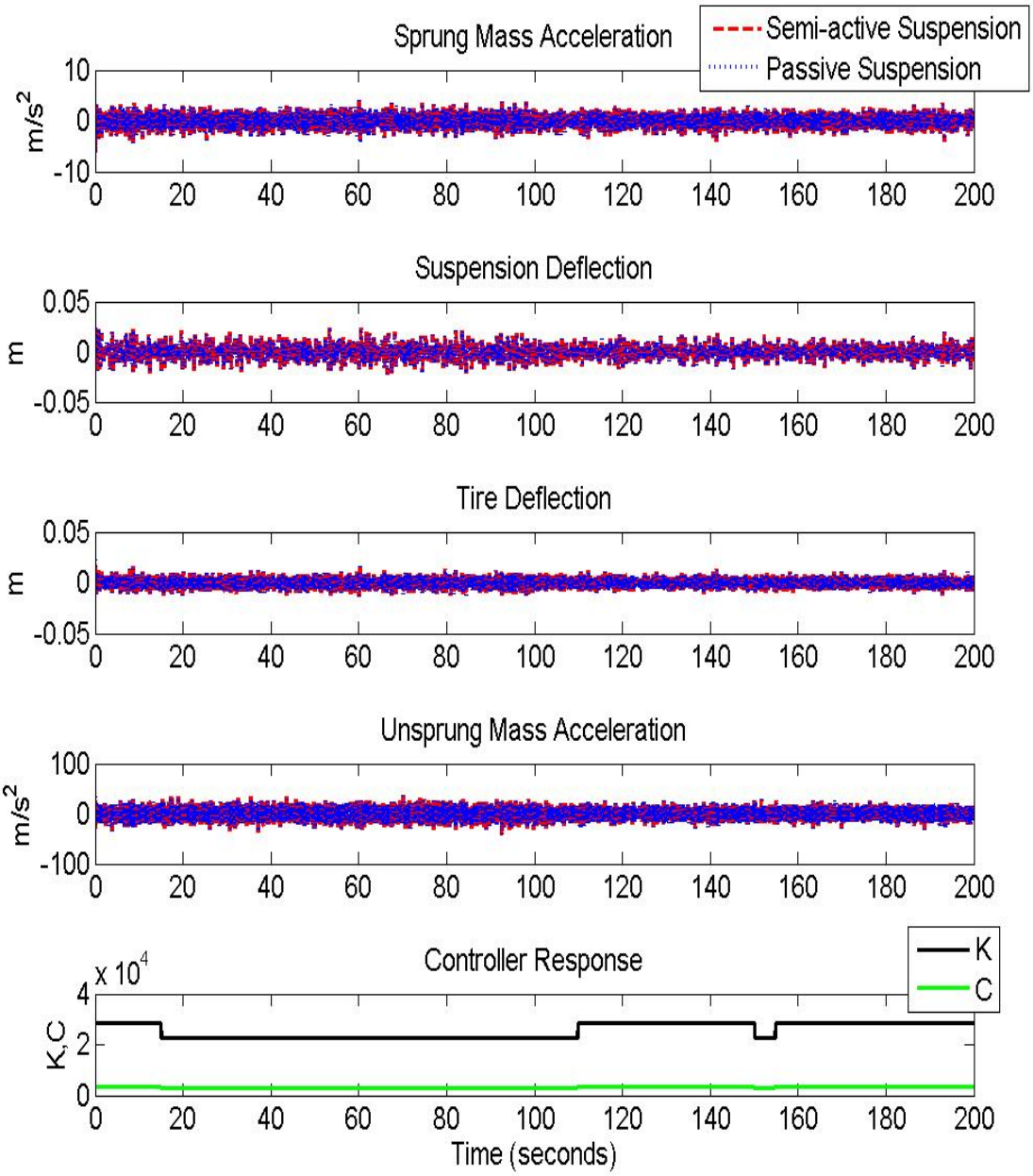

Figure 4-6: Time History and Controller Response at 454.5 kg Sprung Mass traversing Road Course 2

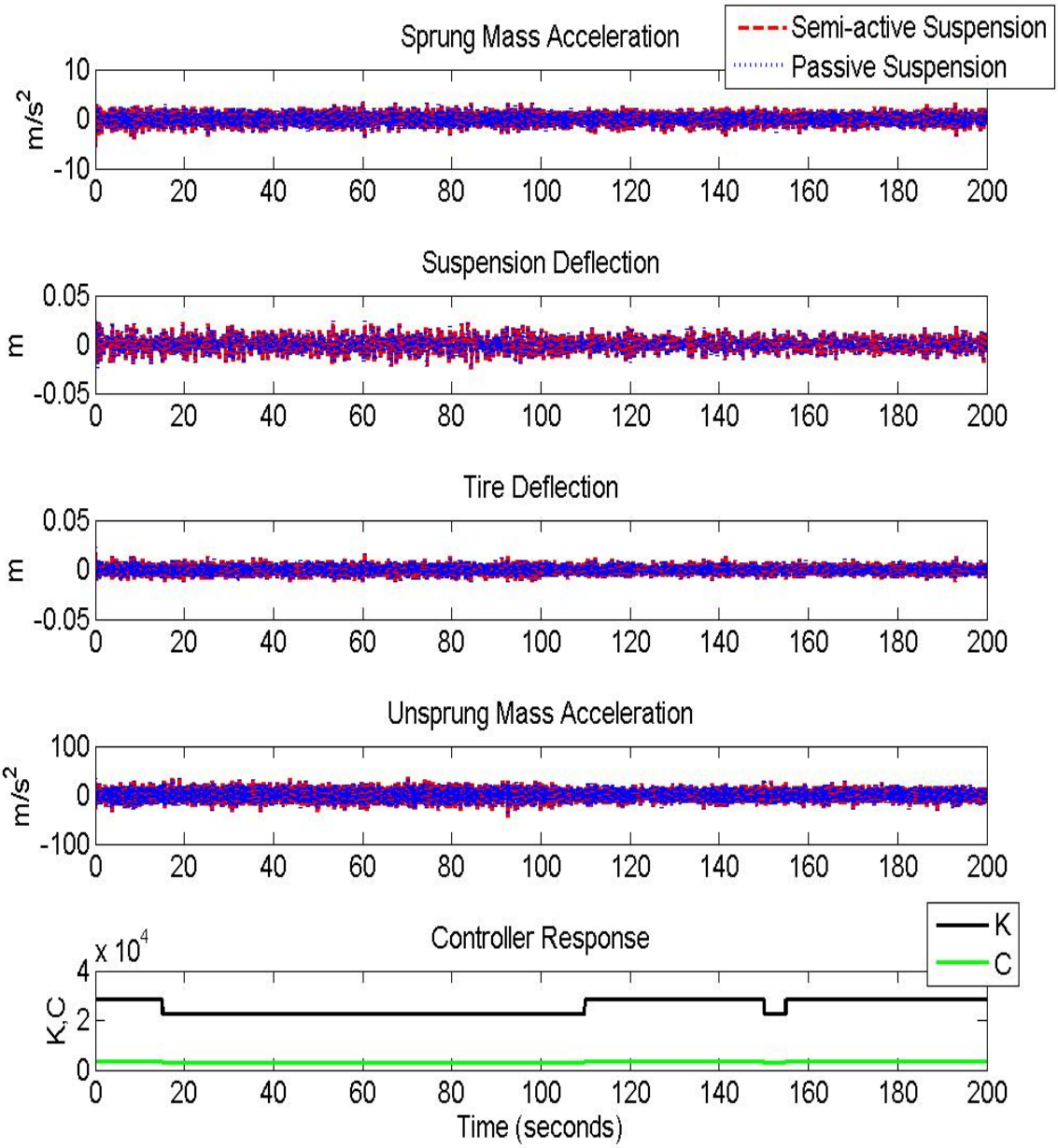

Figure 4-7: Time History and Controller Response at 504.5 kg Sprung Mass traversing Road Course 2

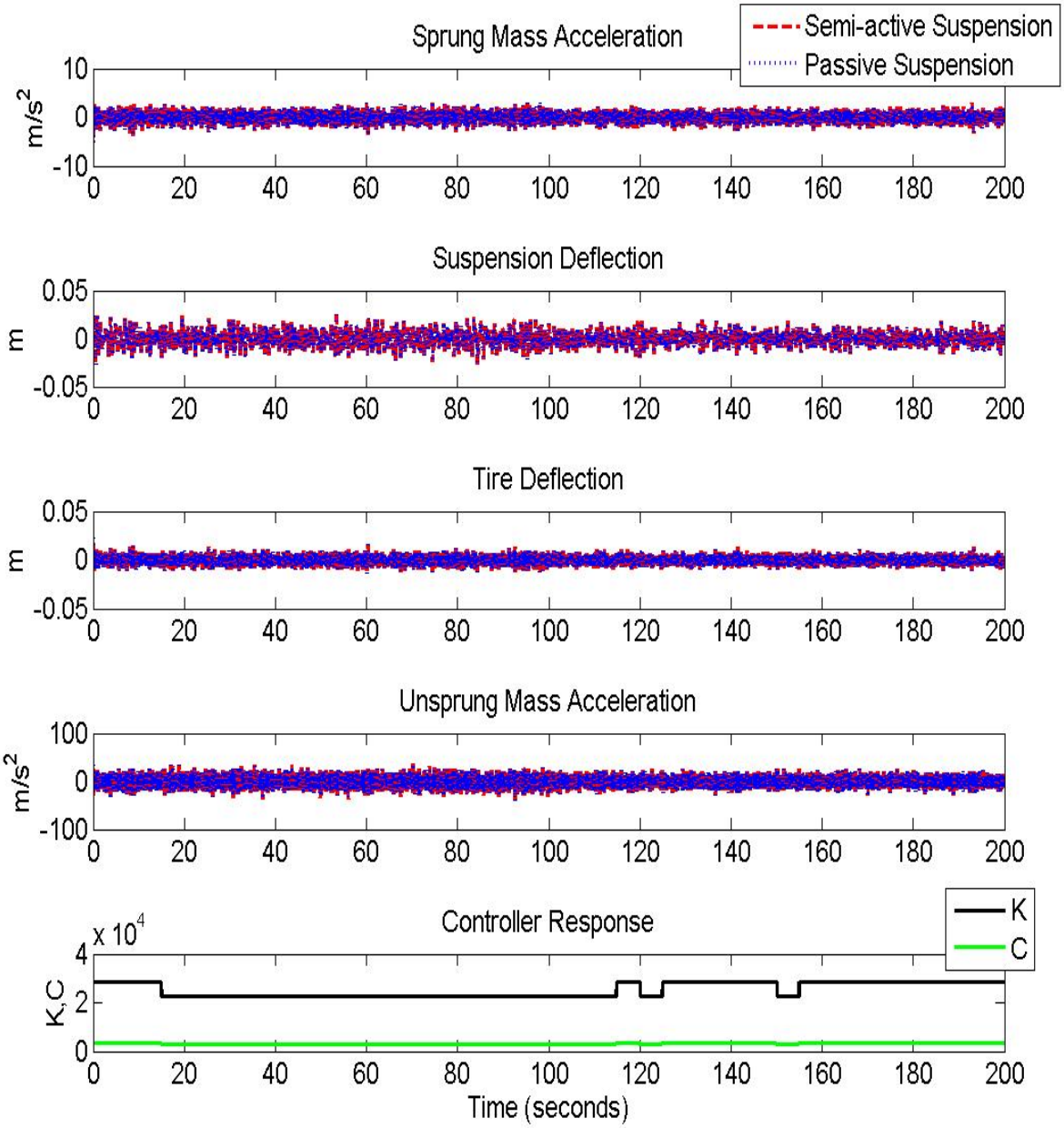

Figure 4-8: Time History and Controller Response at 554.5 kg Sprung Mass traversing Road Course 2

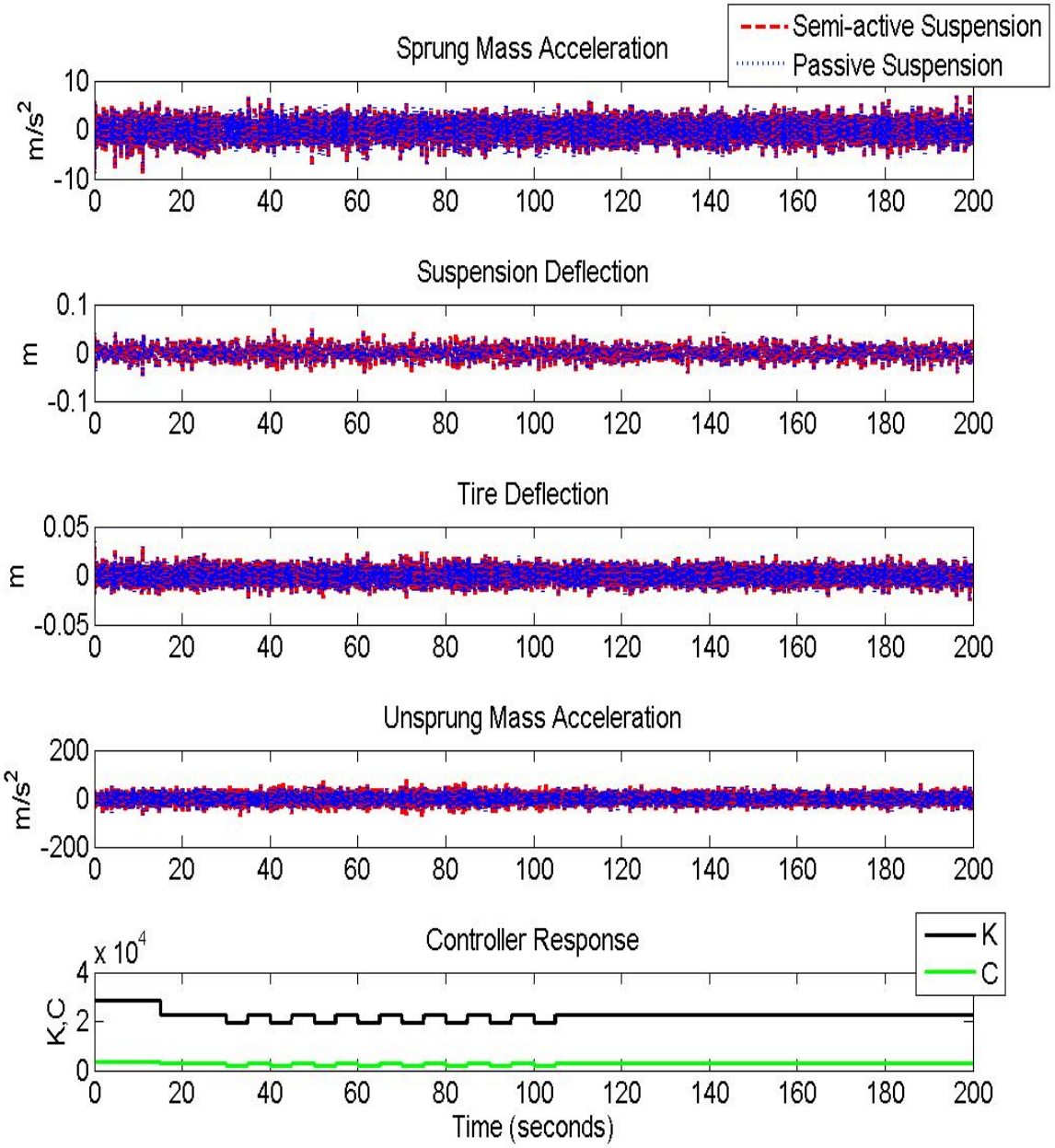

Figure 4-9: Time History and Controller Response at 454.5 kg Sprung Mass traversing Road Course 3

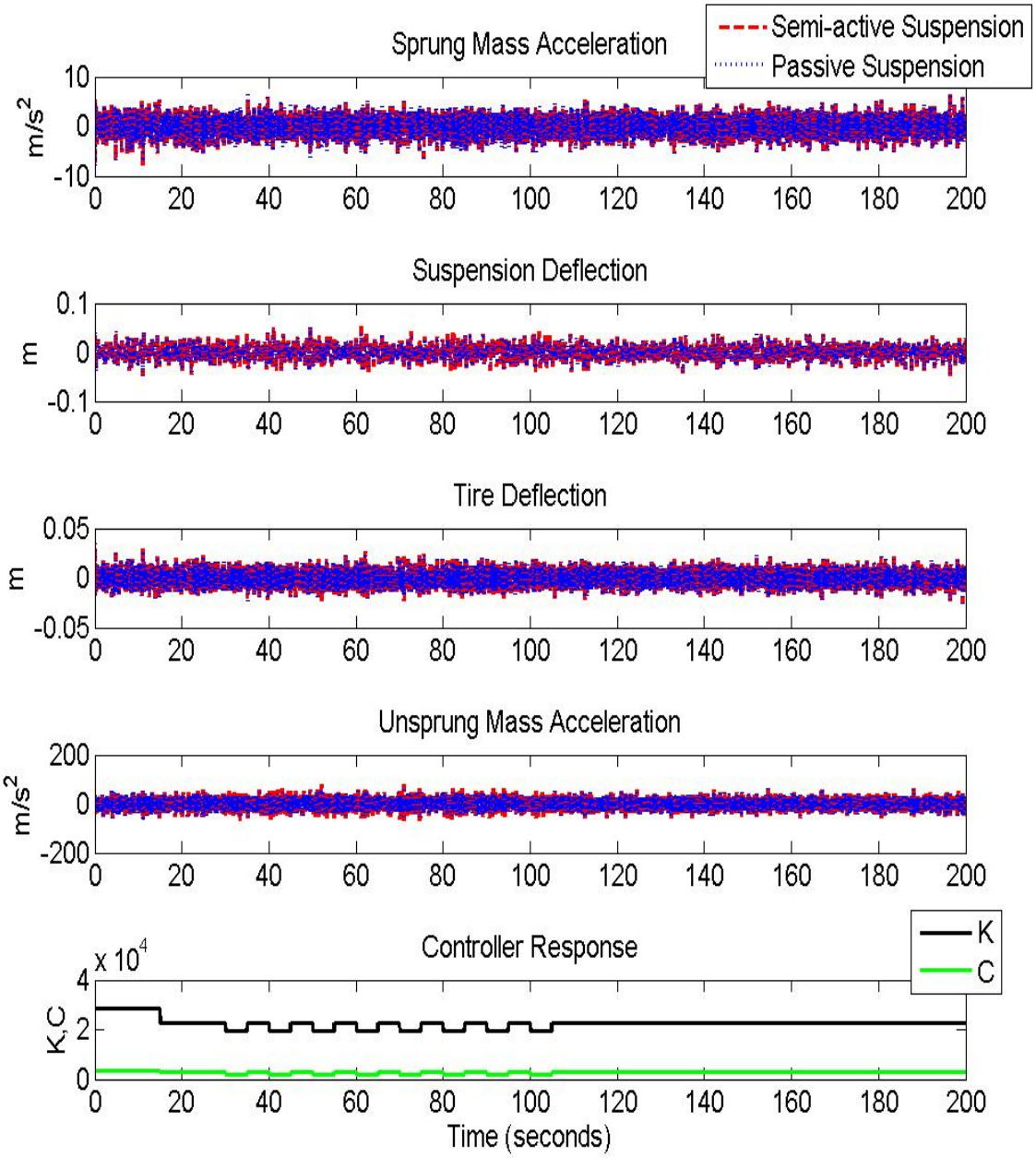

Figure 4-10: Time History and Controller Response at 504.5 kg Sprung Mass traversing Road Course 3

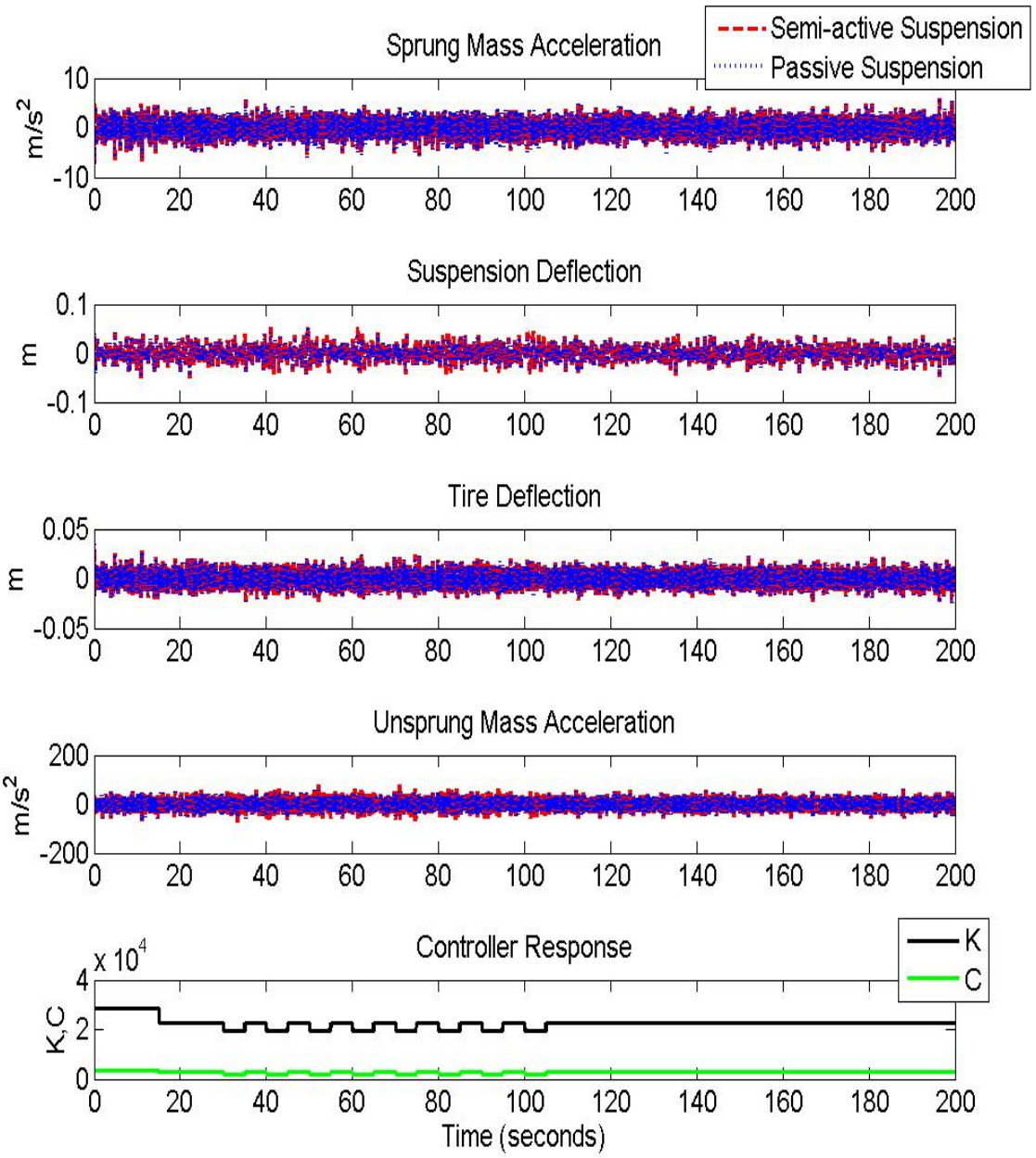

Figure 4-11: Time History and Controller Response at 554.5 kg Sprung Mass traversing Road Course 3

4.2 Vehicle Performance Results and comparison

Table 4-4 to Table 4-30 are the objective vehicle performance RMS metrics (sprung mass acceleration,, suspension deflection, and tire deflection) per each road profile at 454.5, 504.5, and 554.5 kg sprung mass. Note that degraded performance within the tables is represented by negative percentages and vice versa for enhanced performance.

Table 4-4 – Results traversing 1st segment of Road Course 1 at 454.5 kg Sprung Mass

Sprung Mass	Road Course 1 - Segment Road Roughness 4					
454.5kg	RMS Sprung Mass Accel (m/s^2)	RMS Suspension Deflection (m)	RMS Tire Deflection (m)	Percent Improvement from Baseline		
				RMS Sprung Mass Accel	RMS Suspension Deflection	RMS Tire Deflection
Passive Suspension	0.3217	0.0021	0.0011	N/A	N/A	N/A
Semi-Active Suspension	0.3764	0.0018	0.0012	-17.00%	14.29%	-9.09%

Table 4-5 – Results traversing 2nd segment of Road Course 1 at 454.5 kg Sprung Mass

Sprung Mass	Road Course 1 - Segment Road Roughness 256					
454.5kg	RMS Sprung Mass Accel (m/s^2)	RMS Suspension Deflection (m)	RMS Tire Deflection (m)	Percent Improvement from Baseline		
				RMS Sprung Mass Accel	RMS Suspension Deflection	RMS Tire Deflection
Passive Suspension	2.6649	0.0181	0.0089	N/A	N/A	N/A
Semi-Active Suspension	2.3944	0.0208	0.0091	10.15%	-14.92%	2.25%

Table 4-6 – Results traversing Road Course 1 at 454.5 kg Sprung Mass

Sprung Mass	Complete Road Course 1					
454.5kg	RMS Sprung Mass Accel (m/s^2)	RMS Suspension Deflection (m)	RMS Tire Deflection (m)	Percent Improvement from Baseline		
				RMS Sprung Mass Accel	RMS Suspension Deflection	RMS Tire Deflection
Passive Suspension	1.8839	0.0129	0.0063	N/A	N/A	N/A
Semi-Active Suspension	1.7138	0.0148	0.0065	9.03%	-14.73%	-3.17%

Table 4-7 – Results traversing 1st segment of Road Course 1 at 504.5 kg Sprung Mass

Sprung Mass	Road Course 1 - Segment Road Roughness 4					
504.5kg	RMS Sprung Mass Accel (m/s^2)	RMS Suspension Deflection (m)	RMS Tire Deflection (m)	Percent Improvement from Baseline		
				RMS Sprung Mass Accel	RMS Suspension Deflection	RMS Tire Deflection
Passive Suspension	0.2917	0.0022	0.0011	N/A	N/A	N/A
Semi-Active Suspension	0.3405	0.0018	0.0012	-16.73%	18.18	-9.09

Table 4-8 – Results traversing 2nd segment of Road Course 1 at 504.5 kg Sprung Mass

Sprung Mass	Road Course 1 - Segment Road Roughness 256					
504.5kg	RMS Sprung Mass Accel (m/s^2)	RMS Suspension Deflection (m)	RMS Tire Deflection (m)	Percent Improvement from Baseline		
				RMS Sprung Mass Accel	RMS Suspension Deflection	RMS Tire Deflection
Passive Suspension	2.4020	0.0190	0.0089	N/A	N/A	N/A
Semi-Active Suspension	2.1750	0.0218	0.0091	9.45	-14.74	-2.25

Table 4-9 – Results traversing Road Course 1 at 504.5 kg Sprung Mass

Sprung Mass	Complete Road Course 1					
504.5kg	RMS Sprung Mass Accel (m/s^2)	RMS Suspension Deflection (m)	RMS Tire Deflection (m)	Percent Improvement from Baseline		
				RMS Sprung Mass Accel	RMS Suspension Deflection	RMS Tire Deflection
Passive Suspension	1.7109	0.0135	0.0063	N/A	N/A	N/A
Semi-Active Suspension	1.5566	0.0154	0.0065	9.02	-14.07	-3.17

Table 4-10 – Results traversing 1st segment of Road Course 1 at 554.5 kg Sprung Mass

Sprung Mass	Road Course 1 - Segment Road Roughness 4					
554.5kg	RMS Sprung Mass Accel (m/s^2)	RMS Suspension Deflection (m)	RMS Tire Deflection (m)	Percent Improvement from Baseline		
				RMS Sprung Mass Accel	RMS Suspension Deflection	RMS Tire Deflection
Passive Suspension	0.2672	0.0023	0.0011	N/A	N/A	N/A
Semi-Active Suspension	0.3112	0.0019	0.0012	-16.47	17.39	-9.09

Table 4-11 – Results traversing 2nd segment of Road Course 1 at 554.5 kg Sprung Mass

Sprung Mass	Road Course 1 - Segment Road Roughness 256					
554.5kg	RMS Sprung Mass Accel (m/s^2)	RMS Suspension Deflection (m)	RMS Tire Deflection (m)	Percent Improvement from Baseline		
				RMS Sprung Mass Accel	RMS Suspension Deflection	RMS Tire Deflection
Passive Suspension	2.2014	0.0198	0.0089	N/A	N/A	N/A
Semi-Active Suspension	1.9948	0.0227	0.0091	9.38	-14.65	-2.25

Table 4-12 – Results traversing Road Course 1 at 554.5 kg Sprung Mass

Sprung Mass	Complete Road Course 1					
554.5kg	RMS Sprung Mass Accel (m/s^2)	RMS Suspension Deflection (m)	RMS Tire Deflection (m)	Percent Improvement from Baseline		
				RMS Sprung Mass Accel	RMS Suspension Deflection	RMS Tire Deflection
Passive Suspension	1.5680	0.0141	0.0064	N/A	N/A	N/A
Semi-Active Suspension	1.4275	0.0161	0.0065	8.96	-14.18	-1.56

Table 4-13 – Results traversing 1st segment of Road Course 2 at 454.5 kg Sprung Mass

Sprung Mass	Road Course 2 - Segment Road Roughness 45 – 100km/h					
454.5kg	RMS Sprung Mass Accel (m/s^2)	RMS Suspension Deflection (m)	RMS Tire Deflection (m)	Percent Improvement from Baseline		
				RMS Sprung Mass Accel	RMS Suspension Deflection	RMS Tire Deflection
Passive Suspension	1.0970	0.0073	0.0037	N/A	N/A	N/A
Semi-Active Suspension	1.0744	0.0073	0.0037	2.06	0.00	0.00

Table 4-14 – Results traversing 2nd segment of Road Course 2 at 454.5 kg Sprung Mass

Sprung Mass	Road Course 2 - Segment Road Roughness 45 – 60km/h					
454.5kg	RMS Sprung Mass Accel (m/s^2)	RMS Suspension Deflection (m)	RMS Tire Deflection (m)	Percent Improvement from Baseline		
				RMS Sprung Mass Accel	RMS Suspension Deflection	RMS Tire Deflection
Passive Suspension	0.9183	0.0058	0.0031	N/A	N/A	N/A
Semi-Active Suspension	0.9454	0.0056	0.0032	-2.95	3.45	-3.23

Table 4-15 – Results traversing Road Course 2 at 454.5 kg Sprung Mass

Sprung Mass	Complete Road Course 2					
454.5kg	RMS Sprung Mass Accel (m/s^2)	RMS Suspension Deflection (m)	RMS Tire Deflection (m)	Percent Improvement from Baseline		
				RMS Sprung Mass Accel	RMS Suspension Deflection	RMS Tire Deflection
Passive Suspension	1.0116	0.0066	0.0034	N/A	N/A	N/A
Semi-Active Suspension	1.0119	0.0065	0.0034	-0.03	1.52	0.00

Table 4-16 – Results traversing 1st segment of Road Course 2 at 504.5 kg Sprung Mass

Sprung Mass	Road Course 2 - Segment Road Roughness 45 – 100km/h					
504.5kg	RMS Sprung Mass Accel (m/s^2)	RMS Suspension Deflection (m)	RMS Tire Deflection (m)	Percent Improvement from Baseline		
				RMS Sprung Mass Accel	RMS Suspension Deflection	RMS Tire Deflection
Passive Suspension	0.9930	0.0076	0.0037	N/A	N/A	N/A
Semi-Active Suspension	0.9723	0.0076	0.0037	2.08	0.00	0.00

Table 4-17 – Results traversing 2nd segment of Road Course 2 at 504.5 kg Sprung Mass

Sprung Mass	Road Course 2 - Segment Road Roughness 45 – 60km/h					
504.5kg	RMS Sprung Mass Accel (m/s^2)	RMS Suspension Deflection (m)	RMS Tire Deflection (m)	Percent Improvement from Baseline		
				RMS Sprung Mass Accel	RMS Suspension Deflection	RMS Tire Deflection
Passive Suspension	0.8311	0.0060	0.0031	N/A	N/A	N/A
Semi-Active Suspension	0.8558	0.0058	0.0031	-2.97	3.33	0.00

Table 4-18 – Results traversing Road Course 2 at 504.5 kg Sprung Mass

Sprung Mass	Complete Road Course 2					
504.5kg	RMS Sprung Mass Accel (m/s^2)	RMS Suspension Deflection (m)	RMS Tire Deflection (m)	Percent Improvement from Baseline		
				RMS Sprung Mass Accel	RMS Suspension Deflection	RMS Tire Deflection
Passive Suspension	0.9157	0.0068	0.0034	N/A	N/A	N/A
Semi-Active Suspension	0.9159	0.0068	0.0034	-0.02	0.00	0.00

Table 4-19 – Results traversing 1st segment of Road Course 2 at 554.5 kg Sprung Mass

Sprung Mass	Road Course 2 - Segment Road Roughness 45 – 100km/h					
554.5kg	RMS Sprung Mass Accel (m/s^2)	RMS Suspension Deflection (m)	RMS Tire Deflection (m)	Percent Improvement from Baseline		
				RMS Sprung Mass Accel	RMS Suspension Deflection	RMS Tire Deflection
Passive Suspension	0.9079	0.0078	0.0037	N/A	N/A	N/A
Semi-Active Suspension	0.8887	0.0079	0.0037	2.11	-1.28	0.00

Table 4-20 – Results traversing 2nd segment of Road Course 2 at 554.5 kg Sprung Mass

Sprung Mass	Road Course 2 - Segment Road Roughness 45 – 60km/h					
554.5kg	RMS Sprung Mass Accel (m/s^2)	RMS Suspension Deflection (m)	RMS Tire Deflection (m)	Percent Improvement from Baseline		
				RMS Sprung Mass Accel	RMS Suspension Deflection	RMS Tire Deflection
Passive Suspension	0.7596	0.0062	0.0031	N/A	N/A	N/A
Semi-Active Suspension	0.7773	0.0061	0.0031	-2.33	1.61	0.00

Table 4-21 – Results traversing Road Course 2 at 554.5 kg Sprung Mass

Sprung Mass	Complete Road Course 2					
554.5kg	RMS Sprung Mass Accel (m/s^2)	RMS Suspension Deflection (m)	RMS Tire Deflection (m)	Percent Improvement from Baseline		
				RMS Sprung Mass Accel	RMS Suspension Deflection	RMS Tire Deflection
Passive Suspension	0.8370	0.0071	0.0034	N/A	N/A	N/A
Semi-Active Suspension	0.8348	0.0070	0.0034	0.26	1.41	0.00

Table 4-22 – Results traversing 1st segment of Road Course 3 at 454.5 kg Sprung Mass

Sprung Mass	Road Course 3 - Segment Road Roughness 140					
454.5kg	RMS Sprung Mass Accel (m/s^2)	RMS Suspension Deflection (m)	RMS Tire Deflection (m)	Percent Improvement from Baseline		
				RMS Sprung Mass Accel	RMS Suspension Deflection	RMS Tire Deflection
Passive Suspension	1.9125	0.0127	0.0065	N/A	N/A	N/A
Semi-Active Suspension	1.8007	0.0138	0.0066	5.85	-8.66	-1.54

Table 4-23 – Results traversing 2nd segment of Road Course 3 at 454.5 kg Sprung Mass

Sprung Mass	Road Course 3 - Segment Road Roughness 130					
454.5kg	RMS Sprung Mass Accel (m/s^2)	RMS Suspension Deflection (m)	RMS Tire Deflection (m)	Percent Improvement from Baseline		
				RMS Sprung Mass Accel	RMS Suspension Deflection	RMS Tire Deflection
Passive Suspension	1.8127	0.0121	0.0061	N/A	N/A	N/A
Semi-Active Suspension	1.7404	0.0125	0.0061	3.99	-3.31	0.00

Table 4-24 – Results traversing Road Course 3 at 454.5 kg Sprung Mass

Sprung Mass	Complete Road Course 3					
454.5kg	RMS Sprung Mass Accel (m/s^2)	RMS Suspension Deflection (m)	RMS Tire Deflection (m)	Percent Improvement from Baseline		
				RMS Sprung Mass Accel	RMS Suspension Deflection	RMS Tire Deflection
Passive Suspension	1.8632	0.0124	0.0063	N/A	N/A	N/A
Semi-Active Suspension	1.7707	0.0132	0.0063	4.96	-6.45	0.00

Table 4-25 – Results traversing 1st segment of Road Course 3 at 504.5 kg Sprung Mass

Sprung Mass	Road Course 3 - Segment Road Roughness 140					
504.5kg	RMS Sprung Mass Accel (m/s^2)	RMS Suspension Deflection (m)	RMS Tire Deflection (m)	Percent Improvement from Baseline		
				RMS Sprung Mass Accel	RMS Suspension Deflection	RMS Tire Deflection
Passive Suspension	1.7360	0.0134	0.0065	N/A	N/A	N/A
Semi-Active Suspension	1.6350	0.0145	0.0066	5.82	-8.21	-1.54

Table 4-26 – Results traversing 2nd segment of Road Course 3 at 504.5 kg Sprung Mass

Sprung Mass	Road Course 3 - Segment Road Roughness 130					
504.5kg	RMS Sprung Mass Accel (m/s^2)	RMS Suspension Deflection (m)	RMS Tire Deflection (m)	Percent Improvement from Baseline		
				RMS Sprung Mass Accel	RMS Suspension Deflection	RMS Tire Deflection
Passive Suspension	1.6442	0.0127	0.0061	N/A	N/A	N/A
Semi-Active Suspension	1.5769	0.0131	0.0061	4.09	-3.15	0.00

Table 4-27 – Results traversing Road Course 3 at 504.5 kg Sprung Mass

Sprung Mass	Complete Road Course 3					
504.5kg	RMS Sprung Mass Accel (m/s^2)	RMS Suspension Deflection (m)	RMS Tire Deflection (m)	Percent Improvement from Baseline		
				RMS Sprung Mass Accel	RMS Suspension Deflection	RMS Tire Deflection
Passive Suspension	1.6907	0.0130	0.0063	N/A	N/A	N/A
Semi-Active Suspension	1.6062	0.0138	0.0063	5.00	-6.15	0.00

Table 4-28 – Results traversing 1st segment of Road Course 3 at 554.5 kg Sprung Mass

Sprung Mass	Road Course 3 - Segment Road Roughness 140					
554.5kg	RMS Sprung Mass Accel (m/s^2)	RMS Suspension Deflection (m)	RMS Tire Deflection (m)	Percent Improvement from Baseline		
				RMS Sprung Mass Accel	RMS Suspension Deflection	RMS Tire Deflection
Passive Suspension	1.5922	0.0140	0.0065	N/A	N/A	N/A
Semi-Active Suspension	1.4999	0.0152	0.0066	5.80	-8.57	-1.54

Table 4-29 – Results traversing 2nd segment of Road Course 3 at 554.5 kg Sprung Mass

Sprung Mass	Road Course 3 - Segment Road Roughness 130					
554.5kg	RMS Sprung Mass Accel (m/s^2)	RMS Suspension Deflection (m)	RMS Tire Deflection (m)	Percent Improvement from Baseline		
				RMS Sprung Mass Accel	RMS Suspension Deflection	RMS Tire Deflection
Passive Suspension	1.5055	0.0132	0.0061	N/A	N/A	N/A
Semi-Active Suspension	1.4427	0.0137	0.0061	4.17	-3.79	0.00

Table 4-30 – Results traversing Road Course 3 at 554.5 kg Sprung Mass

Sprung Mass	Complete Road Course 3					
554.5kg	RMS Sprung Mass Accel (m/s^2)	RMS Suspension Deflection (m)	RMS Tire Deflection (m)	Percent Improvement from Baseline		
				RMS Sprung Mass Accel	RMS Suspension Deflection	RMS Tire Deflection
Passive Suspension	1.5494	0.0136	0.0063	N/A	N/A	N/A
Semi-Active Suspension	1.4427	0.0145	0.0063	6.89	-6.62	0.00

4.3 Summary

In general, the overall improvements using the semi-active suspension with the lookup table controller appears to be biased or negligible, but in fact there are remarkable improvements when examining the results in segments per the road roughness and vehicle speed. Recalling from the trade-off study, there are performance compromises made in order to achieve greater performance elsewhere depending on the operating condition. For example in road course 2, the overall improvement in performance is generally negligible when comparing the semi-active suspension system to the passive suspension system. This negligible performance is due to the lookup table controller switching suspension state from improving ride comfort to improving suspension deflection, which causes the approximately zero net gain as shown in Table 4-15, Table 4-18, and Table 4-21. Hence, the evaluation of the overall performance gains are distorted by the aggregate road course and should not be used to assess the performance of the semi-active suspension system using the lookup table controller. To evaluate the lookup table controller performance, segments of the road course where the road roughness and vehicle speed is constant should be considered.

When evaluating results depending on segments where the road roughness and vehicle speed are constant, certain performance can be enhanced up to approximately 18%, while compromising other performance by up to 17%. The passive suspension and semi-active suspension have generally similar performances between road roughness for on-road profile B and C, as shown in Table 4-18. The reason for the similarity is because the passive suspension properties are approximately between

the two suspension states for on-road profile B and C within the lookup table controller. When the road roughness for on-road profile A and D are considered, the lookup table controller either significantly improves ride comfort and suspension deflection by approximately 10-20% over the passive suspension system.

In terms of lookup table controller performance, the recognition in change of speed and road roughness can be detected using the preprocessing moving windows. However, the controller has flip-flopping suspension states, which are undesirable, when about the transition RMS values listed in Table 3-8 and shown in Figure 4-9 to Figure 4-11. The temporal deadband appears to be relatively effective, but further enhancement is required to eliminate the flip-flopping effect.

Chapter 5

Conclusions and Future Work

Results from the semi-active suspension exhibits persuasive improvement when compared to passive suspension systems. By managing both stiffness and damping through the lookup table controller, developed in this thesis, vehicle performance of interest can be enhanced by up to 18% over the passive suspension system for a wide range of operating conditions. Likewise, the unimportant vehicle performances are compromised up to 17%. The addition capability of stiffness property management within the controller permits the vehicle's undamped sprung mass natural frequency to vary depending on operating condition, which cannot be achieved by passive suspension systems or conventional semi-active suspension systems that use adjustable dampers. The temporal deadband effectiveness for reducing flip-flopping between neighbouring suspension states appears to operate to some extent, but further enhancement should be formulated to eliminate flip-flopping between neighbouring suspension states.

A key factor in the performance of the lookup table controller is the stochastic based optimization performed off-line to determine the tuned stiffness and damping properties. By means of the Pareto optima set that is produced from the stochastic based optimization, objective trade-off studies can be performed to select stiffness and damping properties depending on the application. In addition, the normalized Pareto surfaces produced from optimization can reveal parameters that are insensitive towards the performance objectives, thus reducing the complexity of the control logic.

In terms of design, the advantage of this controller when compared to conventional semi-active controllers is its ability to enhance vehicle performance for a wide range of operating conditions without the need to frequently adapt the suspension system properties. This may reduce the cost and need for high performance components (i.e. servo-valves), while increasing reliability, through reduced duty cycles, when compared to conventional semi-active suspension systems. In addition, unlike conventional semi-active suspension system, the lookup table controller does not require

absolute velocity measurements for operation. Thus, this semi-active design emerges as a more attractive solution when compared to conventional semi-active suspension systems.

Since the work completed in this thesis used deterministic linear quarter car models for the development of the controller, further controller development is needed for practical implementation. To further enhance robustness of the controller and maintain design simplicity the following future work is proposed:

- Develop and evaluate lookup table controller for vehicle with large sprung mass variation. It is expected that the improvement gains will be larger than for the passenger vehicle. Lookup table controller may require the sprung mass state as an input unlike the mid-size passenger vehicle used for this thesis.
- Addition of statistical deadband, in combination with the temporal deadband, between neighbouring operating conditions to eliminate flip-flopping effects when switching between neighbouring suspension states.
- Use pneumatic spring state equations to validate the optimization results for design purposes. Depending on the volume of pneumatic chambers, the spring characteristic can be highly non-linear and cause vehicle performance to deviate from their linear counterparts. In addition, use relationship between stiffness and pneumatic pressure within each chamber for implementation purposes of the lookup table controller.
- Develop model to capture the transient dynamics when stiffness and damping properties adjust to ensure stable transitioning between lookup table controller states.
- Develop full vehicle model and include performance objectives that are used to evaluate full vehicle models, for example pitch and roll rate, for the optimization of stiffness and damping properties. Taking into account the additional performance objectives will improve the overall controller performance.
- Account for stochastic design parameters during the optimization of stiffness and damping to increase robustness of controller design. Variance in design parameters can degrade vehicle performance unexpectedly.

- Develop robust method for determining road profile. Present preprocessing method for the unsprung mass acceleration signal will be sensitive to white noise, which would exist in practical implementation.

Lastly, it is possible to further enhance the semi-active suspension capabilities by combining the lookup table controller with conventional semi-active controllers, such as Skyhook, to control stiffness and damping, independently, however this may impact cost and reliability.

Bibliography

[1] Khajepour, A., Yin, Z., Cao, D., Ebrahimi, B., "Suspension Systems and Methods with Independent Stiffness and Height Tuning", US pending patent, Application # 13/097,874, and PCT pending patent, Application # CA2011/050262, April 29th, 2011

[2] Yin, Z., Khajepour, A., Cao, D., Ebrahimi, B., "Design and Modelling of a Novel Pneumatic Suspension System", Reports @ university of waterloo, April 10th, 2010

[3] Wong, J.Y., "Theory of Ground Vehicles", 4th edition, John Wiley & Sons, Inc, 2008

[4] Eslaminasab, N., Biglarbeigian, M., Melek, W., and Golnaraghi, M. F., "A Neural Network Based Fuzzy Control Approach to Improve Ride Comfort and Road Handling of Heavy Vehicles Using Semi-Active Dampers" International Journal of Heavy Vehicle Systems, Vol.14, No.2., 2007b

[5] Zargar, B., "Model development, validation and nonlinear control of pneumatic suspensions", PhD thesis, University of Ottawa, 2007

[6] Likaj, R., Shala, A., Bruqi, M., Qelaj, M., "Optimal Design of Quarter Car Vehicle Suspension System", 14th International Research/Expert Conference, 11-18 September, 2010

[7] Sun, T. C., A. C. J. Luo, and H.R. Hamidzadeh, "Dynamic Response and Optimization for Suspension Systems with Non-linear Viscous Damping." ImechE Part K Journal of Multi-body Dynamics 214, 181-187, 2000

[8] Thoresson, M. J., P. E. Uys, P.S. Els, and J.A. Snyman, "Efficient Optimisation of a Vehicle Suspension System, Using a Gradient-based Approximation Method, Part 1: Mathematical Modelling." Mathematical and Computer Modelling, 2009a

[9] Thoresson, M. J., P. E. Uys, P.S. Els, and J.A. Snyma,. "Efficient Optimisation of a Vehicle Suspension System, Using a Gradient-based Approximation Method, Part 2: Optimisation Results." Mathematical and Computer Modelling, 2009b

[10] Yuen, T.J., Ramli, R., “Comparison of Computational Efficiency of MOEA\D and NSGA-II for Passive Vehicle Suspension Optimization”, 24th European Conference on Modelling and Simulation, 2010

[11] Deb, K., A. Pratap, S. Agarwal and T. Meyarivan, "Fast and Elitist Multiobjective Genetic Algorithm: NSGA-II." IEEE Transactions on Evolutionary Computation, Vol. 6, No.2, pp. 182-197, 2002

[12] Zhang, Q. and H. Li, "MOEA/D: A Multiobjective Evolutionary Algorithm Based on Decomposition." IEEE Transactions on Evolutionary Computation, Vol. 11, 2007

[13] Zhang, Q., W. Liu, and H. Li, "The Performance of a New Version of MOEA/D on CEC09 Unconstrained MOP Test Instances." IEEE Congress on Evolutionary Computation, Trondheim, Norway, 2009

[14] Baumal, A. E., J. J. McPhee, and P.H. Calami, "Application of Genetic Algorithms to the Design Optimization of an Active Vehicle Suspension System." Computer Methods in Applied Mechanics and Engineering, Vol. 163, pp. 87-94, 1998

[15] Crosby, M.J., Karnopp, D.C, “The Active Damper”, Shock and Vibration Bulletin, 43, 1973

[16] Eslaminasab, N., “Development of a Semi-active Intelligent Suspension System for Heavy Vehicles”, PhD thesis, University of Waterloo, 2008

[17] Lozoya-Santos, J.J, Morales-Menendez, R., Tudon-Martınez, J.C., Sename, O., Dugard, L., Ramirez-Mendoza, R., “Control Strategies for an Automotive Suspension with a MR Damper”, 18th International Federation of Automatic Control World Congress, 2011.

[18] Badran, S., Salah, A., Abbas, W., Abouelatta, O., “Design of Optimal Linear Suspension for Quarter Car with Human Model using Genetic Algorithms”, Research Bulletin of Jordan ACM, Vol. 2, April 2012

[19] Brach, R. M. and Haddow, A, “On the Dynamic Response of Hydraulic Engine Mounts,” SAE paper, #931321, 1993

[20] Verros, G., Natsiavas, S., and Papadimitriou, C., “Design Optimization of Quarter-car Models with Passive and Semi-active Suspensions under Random Road Excitation,” Journal of Vibration and Control, 11:581-606, 2005

[21] Wong, J.Y., "Theory of Ground Vehicles – 4th edition," John Wiley & Sons , 2008

[22] Gillespie, T., "CarSim Data Manual – Version 5," July 2001

Appendix A

Design Parameter Optimization and Selection

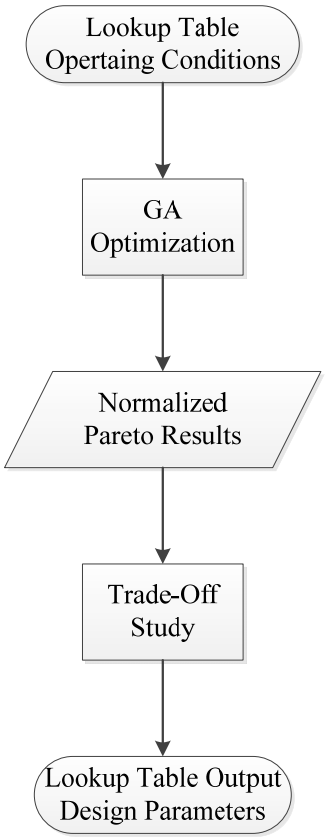

Flow Diagram of Design Parameters selection for Lookup Table Controller

Appendix B

ISO 2631-1:1997 Comfort Weights

Table of ISO weights for comfort evaluation

ISO Weighting for Comfort	
Frequency (Hz)	Weights
0.1	0.0321
0.125	0.0486
0.16	0.079
0.2	0.121
0.25	0.182
0.315	0.263
0.4	0.352
0.5	0.418
0.63	0.459
0.8	0.477
1	0.482
1.25	0.484
1.6	0.494

ISO Weighting for Comfort	
Frequency (Hz)	Weights
2	0.531
2.5	0.631
3.15	0.804
4	0.967
5	1.039
6.3	1.054
8	1.036
10	0.988
12.5	0.902
16	0.768
20	0.636
25	0.513
31.5	0.405

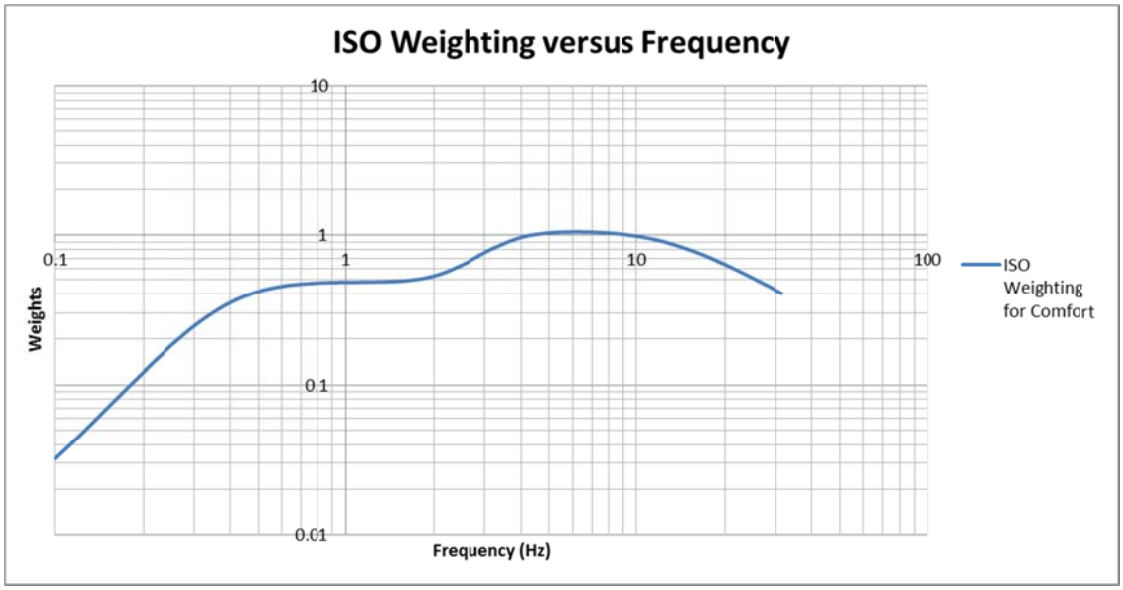

Plot of ISO weights versus Frequency

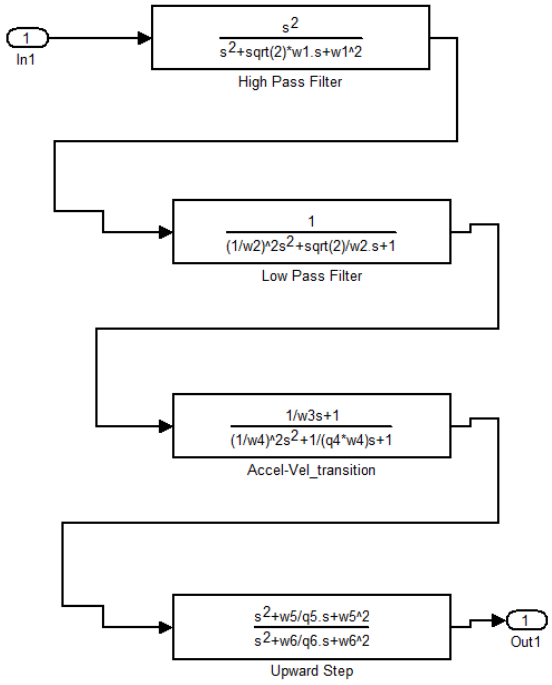


```
Where,

f1=0.4
f2=100
f3=12.5
f4=12.5
q4=0.63
f5=2.37
q5=0.91
f6=3.35
q6=0.91

w1=2*pi*f1
w2=2*pi*f2
w3=2*pi*f3
w4=2*pi*f4
w5=2*pi*f5
w6=2*pi*f6
```

MATLAB/Simulink ISO Comfort Filter

Appendix C

MATLAB/Simulink Lookup Table Controller

```
function KCState_controller(block)
  setup(block);

%endfunction

function setup(block)


  %% Register number of input and output ports
  block.NumInputPorts  = 1;
  block.NumOutputPorts = 1;

  %% Setup functional port properties to dynamically
  %% inherited.
  block.SetPreCompInpPortInfoToDynamic;
  block.SetPreCompOutPortInfoToDynamic;

  block.InputPort(1).Dimensions        = 1;
  block.InputPort(1).DirectFeedthrough = false;

  block.OutputPort(1).Dimensions       = 2;

  %% Set block sample time to inherited
  block.SampleTimes = [0 1];
```

```
  %% Set the block simStateCompliance to default (i.e., same as a built-in block)
  block.SimStateCompliance = 'DefaultSimState';

  %% Register methods
  block.RegBlockMethod('PostPropagationSetup',    @DoPostPropSetup);
  block.RegBlockMethod('InitializeConditions',    @InitConditions);
  block.RegBlockMethod('Outputs',                 @Output);
  block.RegBlockMethod('Update',                  @Update);

%endfunction

function DoPostPropSetup(block)

  %% Setup Dwork
  block.NumDworks = 13;
  block.Dwork(1).Name = 'window';
  block.Dwork(1).Dimensions      = 1;
  block.Dwork(1).DatatypeID      = 0;
  block.Dwork(1).Complexity      = 'Real';
  block.Dwork(1).UsedAsDiscState = true;

  block.Dwork(2).Name = 'x0';
  block.Dwork(2).Dimensions      = 1;
  block.Dwork(2).DatatypeID      = 0;
  block.Dwork(2).Complexity      = 'Real';
  block.Dwork(2).UsedAsDiscState = true;

  block.Dwork(3).Name = 'KC_state1';
  block.Dwork(3).Dimensions      = 2;
```

```
block.Dwork(3).DatatypeID      = 0;
block.Dwork(3).Complexity      = 'Real';
block.Dwork(3).UsedAsDiscState = true;

block.Dwork(4).Name = 'KC_state2';
block.Dwork(4).Dimensions      = 2;
block.Dwork(4).DatatypeID      = 0;
block.Dwork(4).Complexity      = 'Real';
block.Dwork(4).UsedAsDiscState = true;

block.Dwork(5).Name = 'KC_state3';
block.Dwork(5).Dimensions      = 2;
block.Dwork(5).DatatypeID      = 0;
block.Dwork(5).Complexity      = 'Real';
block.Dwork(5).UsedAsDiscState = true;

block.Dwork(6).Name = 'KC_state4';
block.Dwork(6).Dimensions      = 2;
block.Dwork(6).DatatypeID      = 0;
block.Dwork(6).Complexity      = 'Real';
block.Dwork(6).UsedAsDiscState = true;

block.Dwork(7).Name = 'Present_State';
block.Dwork(7).Dimensions      = 1;
block.Dwork(7).DatatypeID      = 0;
block.Dwork(7).Complexity      = 'Real';
block.Dwork(7).UsedAsDiscState = true;

block.Dwork(8).Name = 'flag';
block.Dwork(8).Dimensions      = 1;
block.Dwork(8).DatatypeID      = 0;
```

```
  block.Dwork(8).Complexity      = 'Real';
  block.Dwork(8).UsedAsDiscState = true;

  block.Dwork(9).Name = 'flag2';
  block.Dwork(9).Dimensions      = 1;
  block.Dwork(9).DatatypeID      = 0;
  block.Dwork(9).Complexity      = 'Real';
  block.Dwork(9).UsedAsDiscState = true;

  block.Dwork(10).Name = 'counter';
  block.Dwork(10).Dimensions      = 1;
  block.Dwork(10).DatatypeID      = 0;
  block.Dwork(10).Complexity      = 'Real';
  block.Dwork(10).UsedAsDiscState = true;

% endfunction

function InitConditions(block)

  %% Initialize Dwork
  block.Dwork(1).Data = 1;
  block.Dwork(2).Data = 0;
  block.OutputPort(1).Data = [28475.9616926911;3289.28155202136];
  block.Dwork(3).Data = [19278.6126228466;2022.43280483731];
  block.Dwork(4).Data = [22619.9119314553;2875.51476094665];
  block.Dwork(5).Data = [28475.9616926911;3289.28155202136];
  block.Dwork(6).Data = [35200;4500];
  block.Dwork(7).Data = 3;
  block.Dwork(8).Data = 0;
  block.Dwork(9).Data = 0;
  block.Dwork(10).Data = 1;
```

```
%endfunction

function Output(block)

j = block.Dwork(1).Data;
if j > 1;
  u = evalin('base','u');
end
if block.Dwork(8).Data == 0;
  u(j,:) = block.Dwork(2).Data;
  assignin('base','u',u);
    if j < 1002;
       block.Dwork(1).Data = block.Dwork(1).Data + 1;
    elseif j == 1002;
       block.Dwork(8).Data = 1;
    end
elseif block.Dwork(8).Data == 1;
    if j >= 1002
       u = u((2:1:1002),:);
       u((1002),:) = block.Dwork(2).Data;
       assignin('base','u',u);
       block.Dwork(9).Data = 1;
    end
end

if block.Dwork(8).Data == 1 && block.Dwork(7).Data == 1 && block.Dwork(9).Data == 1;
    [k1,n1] = size(find(abs(u)>20.4));
    [k2,n2] = size(find(abs(u)>10.2));
    [k3,n3] = size(find(abs(u)>5.1));
    if block.Dwork(10).Data == 1;
```

```
    q(block.Dwork(10).Data,:) = k1;
    r(block.Dwork(10).Data,:) = k2;
    s(block.Dwork(10).Data,:) = k3;
    assignin('base','q',q);
    assignin('base','r',r);
    assignin('base','s',s);
    block.Dwork(10).Data = block.Dwork(10).Data + 1;
elseif block.Dwork(10).Data > 1;
    q = evalin('base','q');
    r = evalin('base','r');
    s = evalin('base','s');
    q(block.Dwork(10).Data,:) = k1;
    r(block.Dwork(10).Data,:) = k2;
    s(block.Dwork(10).Data,:) = k3;
    assignin('base','q',q);
    assignin('base','r',r);
    assignin('base','s',s);
    block.Dwork(10).Data = block.Dwork(10).Data + 1;
end
[l1,n1] = size(find(abs(q)>=335));
[l2,n2] = size(find(abs(r)>=335));
[l3,n3] = size(find(abs(s)>=335));
if l1 >= 500 && block.Dwork(10).Data > 500;
    block.OutputPort(1).Data = block.Dwork(3).Data;
    block.Dwork(7).Data = 1;
    block.Dwork(9).Data = 0;
    block.Dwork(10).Data = 1;
    q = 0;
    r = 0;
    s = 0;
    assignin('base','q',q);
```

```
    assignin('base','r',r);
    assignin('base','s',s);
elseif l2 >= 500 && l1 < 501 && block.Dwork(10).Data > 500;
    block.OutputPort(1).Data = block.Dwork(4).Data;
    block.Dwork(7).Data = 2;
    block.Dwork(9).Data = 0;
    block.Dwork(10).Data = 1;
    q = 0;
    r = 0;
    s = 0;
    assignin('base','q',q);
    assignin('base','r',r);
    assignin('base','s',s);
elseif l3 >= 500 && l2 < 500 && l1 < 500 && block.Dwork(10).Data > 500;
    block.OutputPort(1).Data = block.Dwork(5).Data;
    block.Dwork(7).Data = 3;
    block.Dwork(9).Data = 0;
    block.Dwork(10).Data = 1;
    q = 0;
    r = 0;
    s = 0;
    assignin('base','q',q);
    assignin('base','r',r);
    assignin('base','s',s);
elseif l3 < 500 && l2 < 500 && l1 < 500 && block.Dwork(10).Data > 500;
    block.OutputPort(1).Data = block.Dwork(6).Data;
    block.Dwork(7).Data = 4;
    block.Dwork(9).Data = 0;
    block.Dwork(10).Data = 1;
    q = 0;
    r = 0;
```

```
    s = 0;
    assignin('base','q',q);
    assignin('base','r',r);
    assignin('base','s',s);
  end
end

if block.Dwork(8).Data == 1 && block.Dwork(7).Data == 2 && block.Dwork(9).Data == 1;
  [k1,n1] = size(find(abs(u)>16.6));
  [k2,n2] = size(find(abs(u)>8.3));
  [k3,n3] = size(find(abs(u)>4.2));
  if block.Dwork(10).Data == 1;
    q(block.Dwork(10).Data,:) = k1;
    r(block.Dwork(10).Data,:) = k2;
    s(block.Dwork(10).Data,:) = k3;
    assignin('base','q',q);
    assignin('base','r',r);
    assignin('base','s',s);
    block.Dwork(10).Data = block.Dwork(10).Data + 1;
  elseif block.Dwork(10).Data > 1;
    q = evalin('base','q');
    r = evalin('base','r');
    s = evalin('base','s');
    q(block.Dwork(10).Data,:) = k1;
    r(block.Dwork(10).Data,:) = k2;
    s(block.Dwork(10).Data,:) = k3;
    assignin('base','q',q);
    assignin('base','r',r);
    assignin('base','s',s);
    block.Dwork(10).Data = block.Dwork(10).Data + 1;
  end
```

```
[l1,n1] = size(find(abs(q)>=335));
[l2,n2] = size(find(abs(r)>=335));
[l3,n3] = size(find(abs(s)>=335));
if l1 >= 500 && block.Dwork(10).Data > 500;
    block.OutputPort(1).Data = block.Dwork(3).Data;
    block.Dwork(7).Data = 1;
    block.Dwork(9).Data = 0;
    block.Dwork(10).Data = 1;
    q = 0;
    r = 0;
    s = 0;
    assignin('base','q',q);
    assignin('base','r',r);
    assignin('base','s',s);
elseif l2 >= 500 && l1 < 500 && block.Dwork(10).Data > 500;
    block.OutputPort(1).Data = block.Dwork(4).Data;
    block.Dwork(7).Data = 2;
    block.Dwork(9).Data = 0;
    block.Dwork(10).Data = 1;
    q = 0;
    r = 0;
    s = 0;
    assignin('base','q',q);
    assignin('base','r',r);
    assignin('base','s',s);
elseif l3 >= 500 && l2 < 500 && l1 < 500 && block.Dwork(10).Data > 500;
    block.OutputPort(1).Data = block.Dwork(5).Data;
    block.Dwork(7).Data = 3;
    block.Dwork(9).Data = 0;
    block.Dwork(10).Data = 1;
    q = 0;
```

```
        r = 0;
        s = 0;
        assignin('base','q',q);
        assignin('base','r',r);
        assignin('base','s',s);
    elseif l3 < 500 && l2 < 500 && l1 < 500 && block.Dwork(10).Data > 500;
        block.OutputPort(1).Data = block.Dwork(6).Data;
        block.Dwork(7).Data = 4;
        block.Dwork(9).Data = 0;
        block.Dwork(10).Data = 1;
        q = 0;
        r = 0;
        s = 0;
        assignin('base','q',q);
        assignin('base','r',r);
        assignin('base','s',s);
    end
end

if block.Dwork(8).Data == 1 && block.Dwork(7).Data == 3 && block.Dwork(9).Data == 1;
    [k1,n1] = size(find(abs(u)>15.3));
    [k2,n2] = size(find(abs(u)>7.7));
    [k3,n3] = size(find(abs(u)>3.9));
    if block.Dwork(10).Data == 1;
        q(block.Dwork(10).Data,:) = k1;
        r(block.Dwork(10).Data,:) = k2;
        s(block.Dwork(10).Data,:) = k3;
        assignin('base','q',q);
        assignin('base','r',r);
        assignin('base','s',s);
        block.Dwork(10).Data = block.Dwork(10).Data + 1;
```

```
elseif block.Dwork(10).Data > 1;
    q = evalin('base','q');
    r = evalin('base','r');
    s = evalin('base','s');
    q(block.Dwork(10).Data,:) = k1;
    r(block.Dwork(10).Data,:) = k2;
    s(block.Dwork(10).Data,:) = k3;
    assignin('base','q',q);
    assignin('base','r',r);
    assignin('base','s',s);
    block.Dwork(10).Data = block.Dwork(10).Data + 1;
end
[l1,n1] = size(find(abs(q)>=335));
[l2,n2] = size(find(abs(r)>=335));
[l3,n3] = size(find(abs(s)>=335));
if l1 >= 500 && block.Dwork(10).Data > 500;
    block.OutputPort(1).Data = block.Dwork(3).Data;
    block.Dwork(7).Data = 1;
    block.Dwork(9).Data = 0;
    block.Dwork(10).Data = 1;
    q = 0;
    r = 0;
    s = 0;
    assignin('base','q',q);
    assignin('base','r',r);
    assignin('base','s',s);
elseif l2 >= 500 && l1 < 500 && block.Dwork(10).Data > 500;
    block.OutputPort(1).Data = block.Dwork(4).Data;
    block.Dwork(7).Data = 2;
    block.Dwork(9).Data = 0;
    block.Dwork(10).Data = 1;
```

```
        q = 0;
        r = 0;
        s = 0;
        assignin('base','q',q);
        assignin('base','r',r);
        assignin('base','s',s);
    elseif l3 >= 500 && l2 < 500 && l1 < 500 && block.Dwork(10).Data > 500;
        block.OutputPort(1).Data = block.Dwork(5).Data;
        block.Dwork(7).Data = 3;
        block.Dwork(9).Data = 0;
        block.Dwork(10).Data = 1;
        q = 0;
        r = 0;
        s = 0;
        assignin('base','q',q);
        assignin('base','r',r);
        assignin('base','s',s);
    elseif l3 < 500 && l2 < 500 && l1 < 500 && block.Dwork(10).Data > 500;
        block.OutputPort(1).Data = block.Dwork(6).Data;
        block.Dwork(7).Data = 4;
        block.Dwork(9).Data = 0;
        block.Dwork(10).Data = 1;
        q = 0;
        r = 0;
        s = 0;
        assignin('base','q',q);
        assignin('base','r',r);
        assignin('base','s',s);
    end
end
```

```
if block.Dwork(8).Data == 1 && block.Dwork(7).Data == 4 && block.Dwork(9).Data == 1;
   [k1,n1] = size(find(abs(u)>12.3));
   [k2,n2] = size(find(abs(u)>6.2));
   [k3,n3] = size(find(abs(u)>3.1));
   if block.Dwork(10).Data == 1;
      q(block.Dwork(10).Data,:) = k1;
      r(block.Dwork(10).Data,:) = k2;
      s(block.Dwork(10).Data,:) = k3;
      assignin('base','q',q);
      assignin('base','r',r);
      assignin('base','s',s);
      block.Dwork(10).Data = block.Dwork(10).Data + 1;
   elseif block.Dwork(10).Data > 1;
      q = evalin('base','q');
      r = evalin('base','r');
      s = evalin('base','s');
      q(block.Dwork(10).Data,:) = k1;
      r(block.Dwork(10).Data,:) = k2;
      s(block.Dwork(10).Data,:) = k3;
      assignin('base','q',q);
      assignin('base','r',r);
      assignin('base','s',s);
      block.Dwork(10).Data = block.Dwork(10).Data + 1;
   end
   [l1,n1] = size(find(abs(q)>=335));
   [l2,n2] = size(find(abs(r)>=335));
   [l3,n3] = size(find(abs(s)>=335));
   if l1 >= 500 && block.Dwork(10).Data > 500;
      block.OutputPort(1).Data = block.Dwork(3).Data;
      block.Dwork(7).Data = 1;
      block.Dwork(9).Data = 0;
```

```
    block.Dwork(10).Data = 1;
    q = 0;
    r = 0;
    s = 0;
    assignin('base','q',q);
    assignin('base','r',r);
    assignin('base','s',s);
elseif l2 >= 500 && l1 < 500 && block.Dwork(10).Data > 500;
    block.OutputPort(1).Data = block.Dwork(4).Data;
    block.Dwork(7).Data = 2;
    block.Dwork(9).Data = 0;
    block.Dwork(10).Data = 1;
    q = 0;
    r = 0;
    s = 0;
    assignin('base','q',q);
    assignin('base','r',r);
    assignin('base','s',s);
elseif l3 >= 500 && l2 < 500 && l1 < 500 && block.Dwork(10).Data > 500;
    block.OutputPort(1).Data = block.Dwork(5).Data;
    block.Dwork(7).Data = 3;
    block.Dwork(9).Data = 0;
    block.Dwork(10).Data = 1;
    q = 0;
    r = 0;
    s = 0;
    assignin('base','q',q);
    assignin('base','r',r);
    assignin('base','s',s);
elseif l3 < 500 && l2 < 500 && l1 < 500 && block.Dwork(10).Data > 500;
    block.OutputPort(1).Data = block.Dwork(6).Data;
```

```
        block.Dwork(7).Data = 4;
        block.Dwork(9).Data = 0;
        block.Dwork(10).Data = 1;
        q = 0;
        r = 0;
        s = 0;
        assignin('base','q',q);
        assignin('base','r',r);
        assignin('base','s',s);
    end
end

%endfunction

function Update(block)

  block.Dwork(2).Data = block.InputPort(1).Data;

%endfunction
```

Appendix D

Road Courses

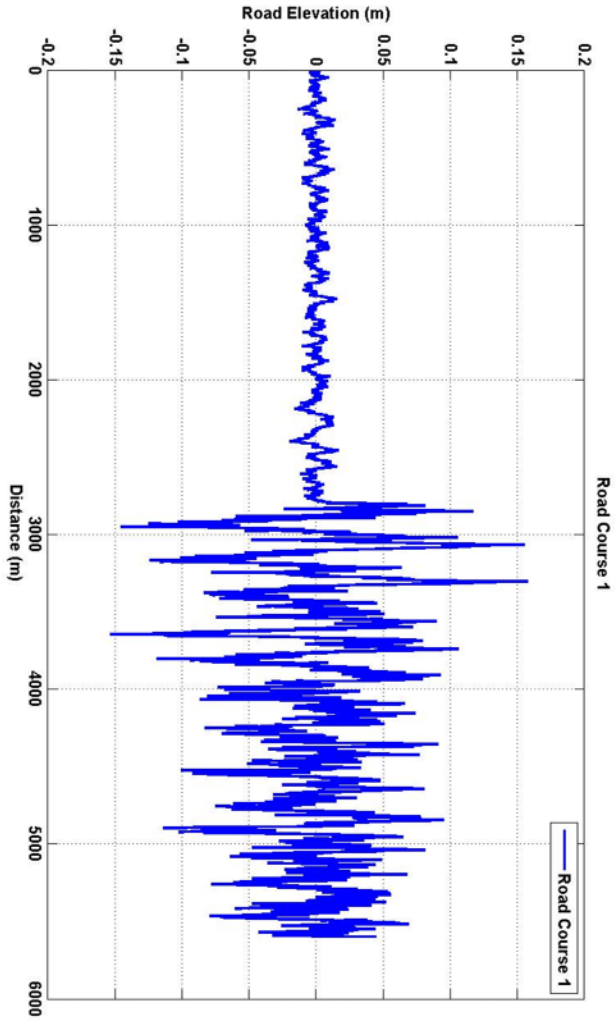

Plot of Road Elevation versus Distance for Road Course 1

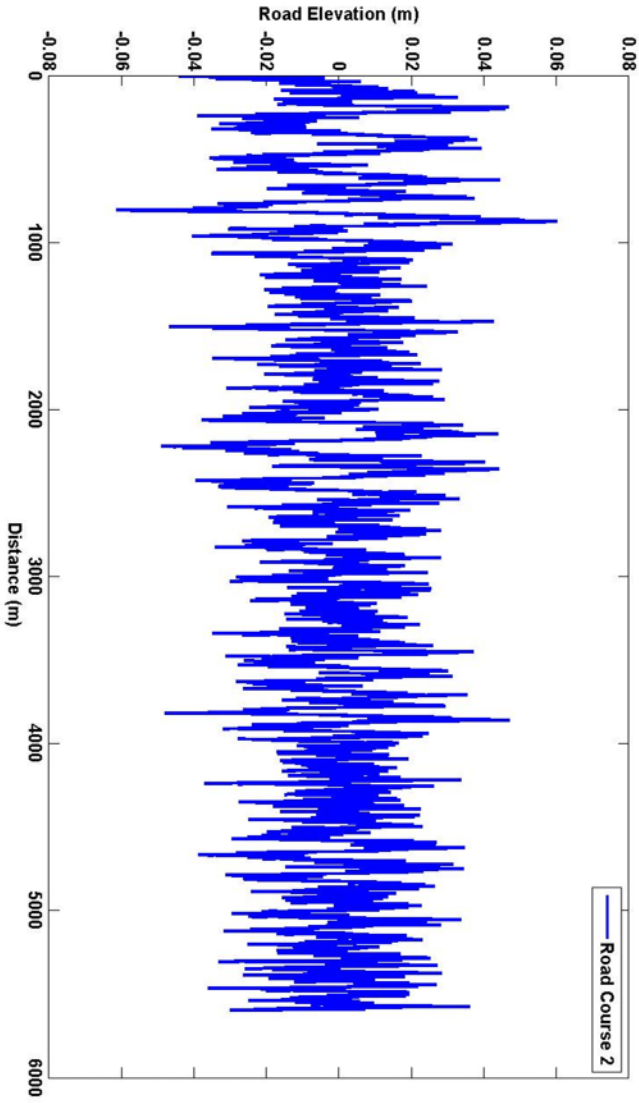

Plot of Road Elevation versus Distance for Road Course 2

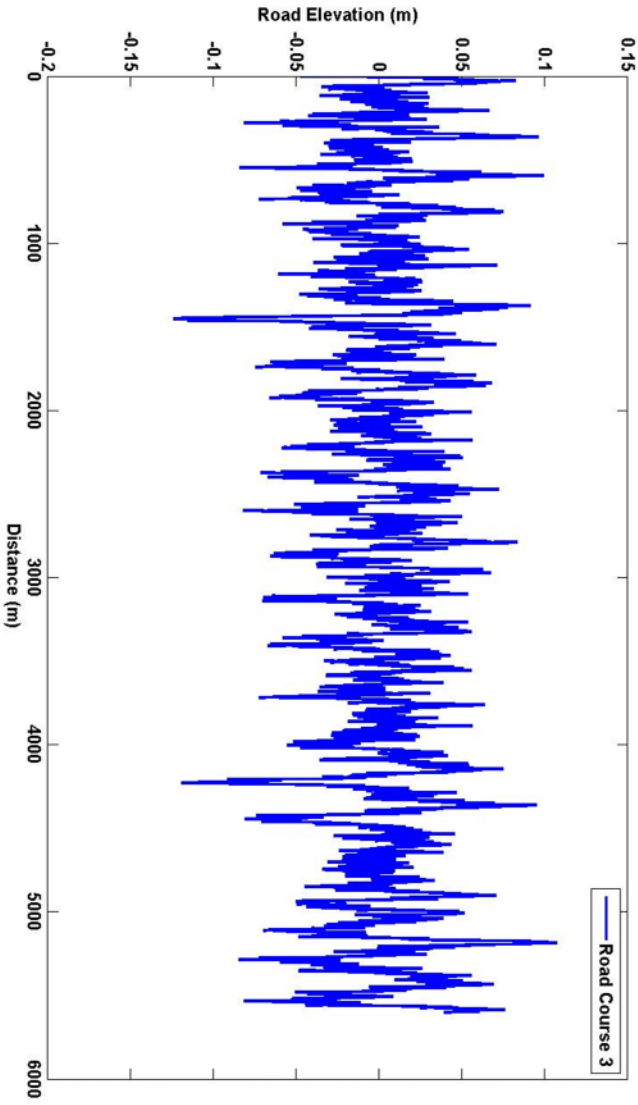

Plot of Road Elevation versus Distance for Road Course 3